Viscoelastic phase separation

2000 J. Phys.: Condens. Matter 12 R207

(http://iopscience.iop.org/0953-8984/12/15/201)

J. Phys.: Condens. Matter **12** (2000) R207–R264. Printed in the UK PII: S0953-8984(00)88541-0

REVIEW ARTICLE

Viscoelastic phase separation

Hajime Tanaka

Institute of Industrial Science, University of Tokyo, Meguro-ku, Tokyo 153-8505, Japan

Received 5 January 2000

Abstract. Descriptions of phase separation in condensed matter have so far been classified into a solid model (model B) and a fluid model (model H). In the former the diffusion is the only transport process, while in the latter material can be transported by both diffusion and hydrodynamic flow. It has recently been found that in addition to these well-known models a new model of phase separation, the 'viscoelastic model', is required to describe the phase-separation behaviour of a dynamically asymmetric mixture, which is composed of fast and slow components. Such 'dynamic asymmetry' can be induced by either the large size difference or the difference in glass-transition temperature between the components of a mixture. The former often exists in so-called complex fluids, such as polymer solutions, micellar solutions, colloidal suspensions, emulsions and protein solutions. The latter, on the other hand, can exist in any mixture in principle. This new type of phase separation is called 'viscoelastic phase separation' since viscoelastic effects play a dominant role. Viscoelastic phase separation may be a 'general' model of phase separation, which includes solid and fluid models as special cases: for example, fluid phase separation described by model H, which is believed to be the usual case, can be viewed as a 'special' (rather rare) case of viscoelastic phase separation. Here we review the experiments, theories and numerical simulations for viscoelastic phase separation. In dynamically asymmetric mixtures, phase separation generally leads to the formation of a long-lived 'interaction network' (a transient gel) of slow-component molecules (or particles), if the attractive interactions between them are strong enough. Because of its long relaxation time, it cannot catch up with the deformation rate of the phase separation itself and as a result the stress is asymmetrically divided between the components. This leads to the transient formation of networklike or spongelike structures of a slow-component-rich phase and its volume shrinking. Domain shape is determined by the force-balance condition in this intermediate stage. However, the true late stage of this phase separation can be described by a fluid model. The process can be viewed as viscoelastic relaxation in pattern formation. We discuss the morphological and kinetic features of viscoelastic phase separation, focusing on the differences from those of usual phase separation. The significance of viscoelastic phase separation in pattern formation in Nature and its engineering applications are also pointed out.

(Some figures in this article appear in colour in the electronic version; see `www.iop.org`)

Contents

1. Introduction

Phase-separation phenomena are widely observed in various kinds of condensed matter including metals, semiconductors, superconductors, simple liquids and complex fluids such as polymers, surfactants, colloids, emulsions and biological materials. The phenomena play key roles in the pattern evolution of immiscible multi-component mixtures of any material. As a result, phase-separation dynamics has been intensively studied in the past three decades from both the fundamental and the industrial viewpoints [1–3]. On the basis of the concept of dynamic universality, descriptions of phase-separation phenomena have been classified into several theoretical models by Hohenberg and Halperin [4] in terms of the type of order parameter and other relevant gross variables: for example, phase separation in solids is known to be described by the 'solid model (model B)', while phase separation in fluids is known to be described by the 'fluid model (model H)' [4]. For the former the local concentration

can be changed only by material diffusion, while for the latter it can be changed by both diffusion and flow. It has been established that within each dynamic universality class the critical and phase-separation behaviour is universal and does not depend upon the details of material properties [1, 2, 4]. This is known as 'dynamic universality', which tells us that the only relevant length scales and timescales are, respectively, the correlation length ξ and the characteristic lifetime τ of the order parameter fluctuations, and all the microscopic details of a system are irrelevant. It is well established that the late-stage coarsening dynamics is beautifully described by the scaling law with the form $R/\xi \sim (t/\tau)^{\alpha}$, where R is the characteristic domain size, t is the phase-separation time and α is the growth exponent. This scaling law is a consequence of the dynamic universality and the self-similar nature of domain growth during phase separation.

In all conventional theories of critical phenomena and phase separation, however, the same dynamics for the two components of a binary mixture, which we call 'dynamic symmetry' between the components, has been implicitly assumed [1, 2, 4]. Also in previous experiments, dynamically symmetric mixtures are most commonly used. For example, a binary liquid mixture is a mixture of components both of which have the fast dynamics, and a polymer blend is a mixture of components both of which have the slow dynamics. These two types of systems are most popularly used to investigate the kinetics of fluid phase separation. The dynamic universality of model H was established by these intensive studies. In particular, the researches on phase separation of a polymer mixture have played quite important roles in our understanding of phase separation [5–9] since its large length scale (large ξ) and long timescale (long τ) make the experimental studies of phase-separation kinetics much easier compared to the case for classical binary liquid mixtures.

Possible polymer effects on phase separation in both stable and unstable states have been explored by many researchers [10–17]. From static aspects, polymer mixtures are known to show mean-field-like behaviour over a wide temperature range, reflecting the long-range bare interaction [18]. From dynamic aspects, on the other hand, viscoelasticity is one of the most significant effects unique to polymer systems [18, 19]. Viscoelastic effects coming from chain entanglements have so far been believed to be important only in the very early stage where the phase-separation time t is shorter than the characteristic viscoelastic time τ_t representing the disentanglement time of a chain [10–13, 18]. Thus the theory based on model H is believed to be valid on timescales longer than τ_t and on spatial scales larger than R_g (R_g: the radius of gyration of a chain). In such a space-time region a system behaves as a viscous fluid and usual phase-separation behaviour should be observed. This picture is very accurate for symmetric mixtures. de Gennes [10] and Pincus [11] suggested the interesting internal mode peculiar to polymeric mixtures for the early stage of spinodal decomposition. However, the experimental study of the above initial viscoelastic regime ($t < \tau_t$) is extremely difficult and there have so far been no experimental reports about this type of viscoelastic effect on phase separation. For the late stage of bicontinuous phase separation, Hashimoto *et al* [6] found the non-universal behaviour which is called N-branching effects. Its mechanism was theoretically explained by Onuki [13]. Pinning effects for droplet coarsening were also suggested to be due to polymer effects arising from the conformational constraint for polymers at the interface [15, 16], although there has as yet been no firm consensus achieved on its physical origin [17]. All these polymer effects reported so far, however, do not originate from the viscoelastic nature of polymers and only weakly affect the phase-separation behaviour. Thus it has been widely believed that the topological characteristics of polymer do not cause any essential change in either the critical dynamics or the phase-separation kinetics and they simply slow down the dynamics due to the large viscosity [6–9, 12, 13, 18]. This was confirmed by extensive studies on polymer mixtures [7, 9] and polymer solutions [20–25]. Thus it was

believed that critical phenomena and phase-separation phenomena for polymeric systems are essentially the same as those for classical fluid mixtures [1, 8, 9].

However, the assumption of dynamic symmetry is hardly valid in various mixtures, especially in a material group of 'complex fluids'. In many cases, complex fluids are mixtures of 'slow' and 'fast' components: e.g., polymer solutions, colloidal suspensions, emulsions, protein solutions and micellar solutions. Complex fluids often exhibit interesting rheological behaviour [26]. Although there were intensive studies on polymer solutions, previous researches mainly focused on the universality [20–25,27] and the effects of dynamic asymmetry were not noticed. Recently, quite unusual phase separation was found in mixtures having intrinsic 'dynamic asymmetry' between their components (e.g., polymer solutions composed of long chainlike molecules and simple liquid molecules) under deep-quench conditions [28–30]. The phase-separation behaviour cannot be explained by the above-described knowledge of the conventional phase separation. In such a mixture, critical concentration fluctuation is not necessarily the only slow mode of the system, contrary to the concept of dynamic universality [31, 32]. It turns out that the interplay between phase-separation (or critical) dynamics and the slow dynamics of the material itself [29–32] plays an important role in the above type of phase separation. More explicitly, the slow fluid component (polymers) cannot catch up with the deformation rate of phase separation itself and starts to behave like a viscoelastic body. Since viscoelastic effects play a crucial role in this phase separation, it is called 'viscoelastic phase separation' [30]. A very similar phenomenon was also observed in a polymer blend, whose components have very different glass-transition temperatures (T_g). This indicates that viscoelastic phase separation is a universal phenomenon common to all dynamically asymmetric mixtures [33]. From the theoretical viewpoint, thus, we need a third general model of phase separation in condensed matter, which we call a 'viscoelastic model' [34], in addition to a solid and a fluid model.

In this review, we show the unique features of viscoelastic phase separation found in experiments and consider their physical mechanisms. The viscoelastic model of phase separation and its universal nature are described in detail. The results of numerical simulations are also briefly reviewed. The relation of viscoelastic phase separation to networklike or spongelike patterns observed in Nature and its industrial applications will also be discussed. Finally we point out some unsolved problems.

2. Usual phase separation

2.1. Phase separation in solid mixtures: the solid model

Before describing the unusual features of viscoelastic phase separation, we briefly review what is known about solid and fluid models of phase separation. As described above, the descriptions of phase separation in isotropic condensed matter have so far been classified into a solid model (model B) and a fluid model (model H) [1]. The only mechanism of transport of material for a solid model is diffusion, namely the exchange of A and B atoms on a lattice. On the other hand, the transport mechanisms for a fluid model are diffusion and hydrodynamic transport.

The kinetic equation of the solid model is [1, 2]

$$\frac{\partial \phi}{\partial t} = \nabla \cdot \left[L(\phi) \nabla \frac{\delta(\beta H)}{\delta \phi} \right] + \theta \tag{1}$$

where L is a transport coefficient, θ is the thermal noise and $\beta = 1/k_B T$ (k_B: Boltzmann's constant). The noise term satisfies the relation

$$\langle \theta(\boldsymbol{r}, t)\theta(\boldsymbol{r}', t') \rangle = -2L \nabla^2 \delta^d(\boldsymbol{r} - \boldsymbol{r}')\delta(t - t') \tag{2}$$

where d is the spatial dimensionality. The ϕ-dependence of L is often neglected, but it is known that it plays an essential role in the problem of phase separation under deep quenching [35,36] and under the effects of external fields (e.g., gravitational fields) [37–40]. It is worth stressing that the ϕ-dependence of L originates from the essence of the diffusion phenomena and should not be neglected in the exact sense. For a dynamically symmetric case, thus, $L(\phi) \propto \phi(1-\phi)$. In the above, H is typically given by the Ginzburg–Landau-type Hamiltonian [1,2]:

$$H = k_{\mathrm{B}}T \int \mathrm{d}\boldsymbol{r}\left[f(\phi) + \frac{C}{2}|\nabla\phi|^2 \right] \tag{3}$$

with

$$f(\phi) = -\frac{r}{2}\phi^2 + \frac{u}{4}\phi^4. \tag{4}$$

Here $r = a(T_{\mathrm{c}} - T)$ (T_{c}: a critical temperature; a: a positive constant) and u and C are positive constants.

2.1.1. The early stage of spinodal decomposition. The early stage of phase separation is described by the Cahn's linear theory [1,2,41]. First we decompose ϕ as $\phi = \bar{\phi} + \delta\phi$ and set $L(\delta\phi) = L + \mathrm{O}(\delta\phi)$. Then, the Fourier component ϕ_q (t) of $\delta\phi(\boldsymbol{r}, t)$ obeys

$$\frac{\partial}{\partial t}\phi_q = -Lq^2(r_{\mathrm{eff}} + Cq^2)\phi_q + \theta_q. \tag{5}$$

Here $r_{\mathrm{eff}} = -r + 3u\bar{\phi}^2$. Thus, the growth rate of ϕ_q is given by $\Gamma_q = Lq^2(r_{\mathrm{eff}} + q^2)$. For negative r_{eff}, long-wavelength fluctuations with $q < |r_{\mathrm{eff}}|^{1/2}$ are unstable. The growth rate Γ_q has a maximum at $q_m = |\frac{1}{2}r_{\mathrm{eff}}|^{1/2}$. Thus, the structure factor $S(q)$ has a peak at q_m and its peak intensity grows exponentially with a rate of $2\Gamma_q = L|r_{\mathrm{eff}}|^2/2$.

2.1.2. Nucleation and growth. The simplest theory describing the nucleation–growth-type phase separation is the Lifshitz–Slyozov–Wagner theory [1, 2, 41–43], which deals with the case of a very small volume fraction of the nucleating phase, $\Phi_{\mathrm{n}}(t) \sim 0$. This mean-field theory is valid also for fluid mixtures for $\Phi_{\mathrm{n}}(t) \leqslant 0.01$. The droplet coarsening is due to the diffusion flux induced by the concentration gradient of the matrix phase around droplets, which is determined by the Gibbs–Thomson relation. The coarsening law in this case is known to be $R(t) = R_{\mathrm{c}}(0)[\frac{4}{9}\Gamma_{\mathrm{c}}(0)t]^{1/3}$, where R_{c} is the critical radius for nucleation and Γ_{c} is the growth rate of a critical nucleus. Γ_{c} is given by $\Gamma_{\mathrm{c}} = 2Dd_0/R_{\mathrm{c}}^3 = (\frac{1}{4}Dd_0^{-2})\Delta^3$, where D is the diffusion constant and d_0 is the capillary length, given by $d_0 = \sigma/(8k_{\mathrm{B}}T\phi_{\mathrm{e}}^2\kappa^2)$ (σ: interfacial tension; $2\phi_{\mathrm{e}}$: the concentration difference between the two coexisting phases; κ: the inverse of the interface thickness, or the correlation length, ξ) and Δ is the degree of supersaturation.

2.1.3. The late stage of phase separation: self-similar growth and scaling laws. In the late stage, it is well known that the peak wavenumber of the structure factor $S(q)$, q_{p}, obeys the following scaling law: $q_{\mathrm{p}}(t) \propto t^{-\alpha}$. The late-stage coarsening can be discussed with the local equilibrium assumption and the theory of interface dynamics [1,2,41,44]. The former ensures the self-similarity of the domain growth, which leads to the conclusion that there is only one length scale (domain size) in our problem. Thus, the scaled structure factor collapses onto a single master curve. The latter, on the other hand, tells us that the jump in the diffusion flux at the interface leads to the motion of the interface. For a solid model, thus, we obtain $R^3 \sim D_\xi \xi t$ (D_ξ: a characteristic diffusion constant; ξ: the correlation length); that is, $\alpha = 1/3$.

2.2. Phase separation in fluid mixtures: the fluid model

For a solid system the only gross variable is the composition ϕ, while for a fluid system the gross variables are ϕ and the velocity field $\boldsymbol{v}$. Thus the kinetic equations for classical binary fluids (model H in the Hohenberg–Halperin notation [4]) are [1, 2, 4, 45]

$$\frac{\partial \phi}{\partial t} = -\boldsymbol{\nabla} \cdot (\phi \boldsymbol{v}) + L \boldsymbol{\nabla}^2 \frac{\delta(\beta H)}{\delta \phi} + \theta \tag{6}$$

$$\rho \frac{\partial \boldsymbol{v}}{\partial t} \cong \boldsymbol{F}_\phi - \boldsymbol{\nabla} p + \eta \boldsymbol{\nabla}^2 \boldsymbol{v} + \boldsymbol{\iota} \tag{7}$$

where ρ is the density, p is a part of the pressure, η is the viscosity, θ and $\boldsymbol{\iota}$ are, respectively, the thermal composition and force noises. Note that the transport coefficient L is the renormalized one [14]. Here the noise terms θ and $\boldsymbol{\iota}$ satisfy, respectively, the fluctuation-dissipation relations, equation (2), and

$$\langle \zeta_i(\boldsymbol{r}, t) \zeta_j(\boldsymbol{r}', t') \rangle = -2\eta \delta_{ij} \boldsymbol{\nabla}^2 \delta^d(\boldsymbol{r} - \boldsymbol{r}') \delta(t - t'). \tag{8}$$

In equation (7), $\boldsymbol{F}_\phi$ is the thermodynamic force density acting on the fluid due to the fluctuations of the composition ϕ that is given by

$$\frac{\boldsymbol{F}_\phi}{k_{\mathrm{B}} T} = -\boldsymbol{\nabla} \cdot \boldsymbol{\Pi} = -\phi \boldsymbol{\nabla} \mu. \tag{9}$$

Here $\boldsymbol{\Pi}$ is the osmotic stress tensor and

$$\Pi_{ij} = \delta_{ij} \left(\pi - \frac{1}{2} C |\nabla \phi|^2 - C \phi \nabla^2 \phi \right) + C \frac{\partial \phi}{\partial x_i} \frac{\partial \phi}{\partial x_j} \tag{10}$$

where π is the osmotic pressure given by $\pi = \phi(\partial f / \partial \phi) - f$ and $\mu = \delta(\beta H)/\delta \phi$ is the chemical potential. In the above, we assume that the viscosity is the same for the two components of a fluid mixture (dynamic symmetry), for simplicity. The first term on the right-hand side of equation (6) is the streaming term, which represents the hydrodynamic transport of composition ϕ. The characteristic feature of a fluid system is that the velocity field $\boldsymbol{v}(\boldsymbol{r}, t)$ strongly affects the dynamics with the coupling to $\phi(\boldsymbol{r}, t)$. If we set $\boldsymbol{v} = \boldsymbol{0}$ in equation (6), a basic equation for solid systems (model B [4]) is obtained.

Since the above coupled equations are difficult to solve as they are, the equations are usually simplified, using the steady-state approximation. The pressure p in equation (7) is determined so as to satisfy the incompressibility condition $\boldsymbol{\nabla} \cdot \boldsymbol{v} = 0$, which should be satisfied for slow hydrodynamic modes of phase separation in fluid mixtures since they are much slower than sound modes.

The steady-state approximation ($\partial \boldsymbol{v}/\partial t \sim 0$) leads to the following expression for $\boldsymbol{v}$ [1,14] under the condition $\boldsymbol{\nabla} \cdot \boldsymbol{v} = 0$:

$$\boldsymbol{v} = \int \mathrm{d}\boldsymbol{r}' \, \boldsymbol{T}(\boldsymbol{r} - \boldsymbol{r}') \cdot [\boldsymbol{F}_\phi(\boldsymbol{r}') + \boldsymbol{\iota}(\boldsymbol{r}')]. \tag{11}$$

Here $\boldsymbol{T}$ is the so-called Osceen tensor given by

$$\boldsymbol{T}(\boldsymbol{r}) = \frac{1}{8\pi\eta r} \left(\boldsymbol{I} + \frac{\boldsymbol{r}\boldsymbol{r}}{r^2} \right) \tag{12}$$

where $\boldsymbol{I}$ is the unit tensor and $r = |\boldsymbol{r}|$. Thus, only one equation (equation (6) with $\boldsymbol{v}$ expressed by equation (11)) is necessary to describe phase separation of incompressible fluid mixtures for a case with $\partial \boldsymbol{v}/\partial t \sim 0$ [14].

2.2.1. The early stage of phase separation. The early-stage phase separation is essentially the same as in the solid model. The (i) spinodal decomposition and (ii) nucleation and growth are described by Cahn's linear theory and the Lifshitz–Slyozov theory, respectively. The velocity fields are induced by the motion of a rather sharp interface and, thus, not important in the initial stage of spinodal decomposition even for bicontinuous phase separation. Note that the average velocity grows as $\delta\phi^2$, where $\delta\phi$ is the amplitude of the composition fluctuations. Further, they do not play important roles in the nucleation and growth process because of the divergent character of the $\boldsymbol{n}$-pattern (see section 2.2.2 on its definition) and large distances between nuclei, which ensure rare collisions between nuclei.

2.2.2. The late stage of phase separation: self-similar growth and scaling laws. The above interface-tension-induced velocity fields (see equation (11)) give us physical insight into hydrodynamic effects on domain coarsening as follows (see, e.g., references [2, 41, 44]). After the formation of a sharp interface, the interface profile can be approximately described by the local equilibrium composition profile of an interface, $\phi_{\rm int} = \phi_{\rm e}\tanh(\zeta/\sqrt{2}\xi)$, where $\phi_{\rm e}$ $(=\sqrt{|r|/u})$ is the equilibrium composition and ξ is the correlation length ($\xi = \sqrt{C/|r|}$). ζ is the distance from the interface defined by $\zeta = \boldsymbol{n}\cdot(\boldsymbol{r}-\boldsymbol{r}_a)$, where $\boldsymbol{r}_a$ is a point on the interface and $\boldsymbol{n}$ is the unit normal vector at the point $\boldsymbol{r}_a$ toward the domain with a positive value of ϕ. Then, the thermodynamic force density due to interface $\boldsymbol{F}_\phi^{\rm int}$ can be expressed by

$$\frac{\boldsymbol{F}_\phi^{\rm int}}{k_{\rm B}T} = -C\,\boldsymbol{\nabla}^2\phi\,\boldsymbol{\nabla}\phi = -C(\boldsymbol{\nabla}\cdot\boldsymbol{n})\left(\frac{\partial\phi_{\rm int}}{\partial\zeta}\right)^2\boldsymbol{n}. \tag{13}$$

Note that the conserved part of the force cannot produce any velocity fields for an incompressible fluid and should be balanced with the pressure p. Here $\boldsymbol{\nabla}\cdot\boldsymbol{n}$ is the curvature at $\boldsymbol{r}_a$ and $\boldsymbol{\nabla}\cdot\boldsymbol{n} = 1/R_1 + 1/R_2$, where $1/R_1$ and $1/R_2$ are the two principal curvatures of the interface. Here we use the relations

$$\boldsymbol{\nabla}\phi \cong (\partial\phi_{\rm int}/\partial\zeta)\boldsymbol{n} \qquad \boldsymbol{\nabla}^2\phi \cong \frac{\partial^2\phi_{\rm int}}{\partial\zeta^2} + \left(\frac{\partial\phi_{\rm int}}{\partial\zeta}\right)\boldsymbol{\nabla}\cdot\boldsymbol{n}. \tag{14}$$

Thus, we obtain the following equation by putting equation (13) into equation (7) and using the relation $k_{\rm B}TC(\partial\phi_{\rm int}/\partial\zeta)^2 \cong \sigma\delta(\zeta)$ where σ is the interface tension:

$$-\boldsymbol{\nabla}p' - \sigma\left(\frac{1}{R_1}+\frac{1}{R_2}\right)\delta(\zeta)\boldsymbol{n} + \eta\,\boldsymbol{\nabla}^2\boldsymbol{v} + \boldsymbol{\iota} = 0. \tag{15}$$

Under the incompressibility condition, *the domain geometry*, which we call the '$\boldsymbol{n}$-pattern', selects the coarsening mechanism. Thus we consider bicontinuous phase separation of symmetric fluid mixtures and droplet phase separation of off-symmetric fluid mixtures separately. Typical pattern-evolution processes for bicontinuous and droplet spinodal decomposition are shown in figure 1. In both cases, the most important concept is the self-similar growth of domains, which ensures the existence of only one length scale, namely, the domain size R.

(A) *Bicontinuous phase separation of symmetric fluid mixtures.* For a symmetric composition ($\Phi_{\rm A} \sim 1/2$; $\Phi_{\rm A}$: the volume fraction of the A-rich phase), the second term in equation (15) produces the velocity fields with $v \sim \sigma/\eta$ that lead to the growth law $R \sim (\sigma/\eta)t$ (Siggia's mechanism [46]). The scaled version is $R/\xi = b_{\rm h}(t/\tau)$, where $b_{\rm h}$ is a universal constant. This is because the non-divergent character of the $\boldsymbol{n}$-pattern of a bicontinuous structure allows the second term of equation (15) to directly produce the velocity fields even under the incompressibility condition. The resulting velocity fields $\boldsymbol{v}(\boldsymbol{r})$ are given by

$$\boldsymbol{v}(\boldsymbol{r}) \sim \int \mathrm{d}a\; \boldsymbol{T}(\boldsymbol{r}-\boldsymbol{r}_a)\cdot\boldsymbol{n}(\boldsymbol{r}_a)\sigma\left(\frac{1}{R_1}+\frac{1}{R_2}\right)_a \tag{16}$$

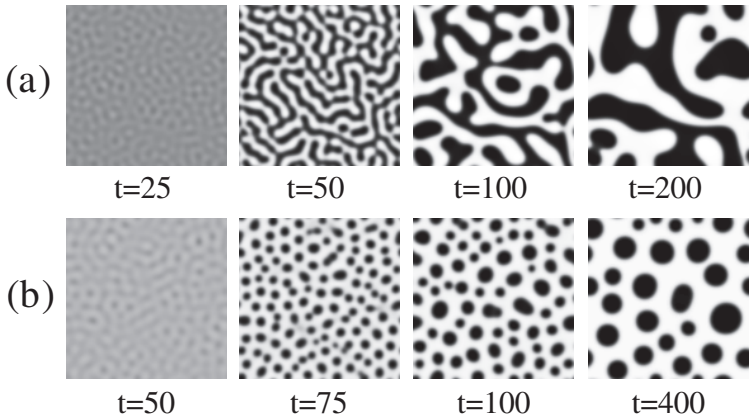

Figure 1. Typical phase-separation processes for (a) bicontinuous and (b) droplet spinodal decomposition in a two-dimensional fluid mixture. They are simulated by numerically solving the basic equations of model H. Time is scaled by the characteristic time τ.

where $\boldsymbol{r}_a$ is a point on the domain interface, da is the area element of the interface and $(1/R_1+1/R_2)_a$ is the mean curvature of the interface at $\boldsymbol{r}_a$. Thus, the geometrical deviation from the minimal surface where $(1/R_1 + 1/R_2)_a = 0$ everywhere is the driving force of the velocity fields.

(B) *Droplet phase separation of off-symmetric fluid mixtures.* For an off-symmetric composition ($\Phi_A \neq \sim 1/2$), on the other hand, the $\boldsymbol{n}$-pattern of droplet morphology has a divergent character. Thus, the second term in equation (15) has to be balanced with $\boldsymbol{\nabla} p$ to satisfy $\boldsymbol{\nabla} \cdot \boldsymbol{v} = 0$ and cannot produce any velocity fields. Accordingly, there is a pressure difference of $2\sigma/R$ across the interface (Laplace's law), while there are no macroscopic velocity fields ($\boldsymbol{v} = 0$) and no interparticle interactions. The latter fact is the basis of the Brownian-coagulation mechanism, which assumes that there are no interparticle interactions and the droplet motion is driven purely by thermal force noises $\boldsymbol{\iota}$ in equation (7). In this case, the domain coarsening is driven by a hydrodynamic diffusion process of droplets. By considering diffusion of a droplet of size R over the interdroplet distance $\sim R$, we straightforwardly obtain $R^2 \sim D_R t$, where $D_R \sim k_B T/(5\pi\eta R)$. This leads to the coarsening law $R \sim (k_B T/\eta)^{1/3} t^{1/3}$. The scaled version is $R/\xi = b_d (t/\tau)^{1/3}$, where b_d is a universal constant. This mechanism is well known as the Brownian-coagulation (Binder–Stauffer) mechanism [46–48]. It should be noted that there may exist some additional mechanisms of droplet coarsening in fluid mixtures [49–52], which originate from the coupling of composition (diffusion) and velocity fields.

2.3. Universality

Since the late-stage scaling law is universal in nature, it should be common to all systems, as long as they belong to the same dynamic universality class. This is well confirmed by extensive experimental studies [1]. For example, phase separation of polymer mixtures and classical binary fluid mixtures is described by the scaling laws of model H described above [8,9]. Here we mention some minor correction required for the description of polymer mixtures, which weakly violates the dynamic universality. This is known as the N-branching effect (N: the degree of polymerization) [6, 13]. This originates from the fact that for a polymer blend the interface tension σ depends not only on ξ but also on N. In the case of a polymer blend, the

interfacial tension near the critical point but still in the mean-field regime can be approximated by [53, 54]

$$\sigma = \frac{2}{3} k_B T b^{-2} N^{-1/2} \epsilon^{3/2} \tag{17}$$

where b is the statistical segment length and $\epsilon = (T - T_c)/T_c$. This leads to the weak N-dependence of b_h for Siggia's mechanism [13]. It should be stressed, however, that Siggia's mechanism itself holds well. Thus, the universality can be recovered by making a correction to the numerical factor b_h.

Here we summarize the common-sense view of phase separation, taking polymer solutions as an example (see figure 2). As described above, the phase-separation kinetics has been classified into three types without any exception: bicontinuous and droplet spinodal decomposition in the unstable region and nucleation–growth-type phase separation in the metastable region. Thus, the manner of phase separation has been believed to be controlled solely by the initial composition of a mixture, namely, the 'static composition symmetry'. In the following, we will show that this well-accepted view is not necessarily correct for dynamically asymmetric mixtures (see figure 6).

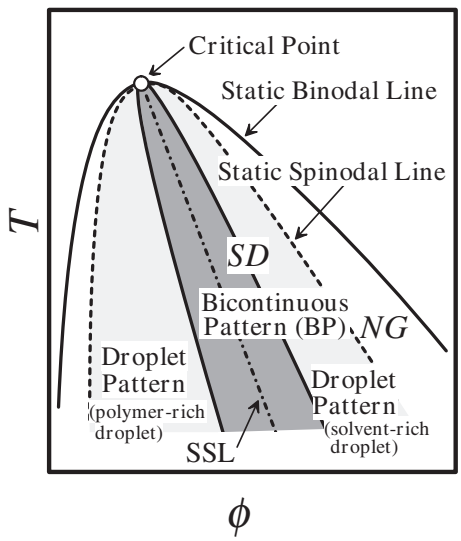

Figure 2. A typical phase diagram of fluid mixtures: polymer solutions as an example. Depending upon the composition symmetry, various types of phase separation are observed. SSL stands for static symmetry line.

3. Viscoelastic phase separation: experimental evidence

Here we describe unusual phase-separation behaviour found in two types of dynamically asymmetric mixture. Since there have so far been few studies on viscoelastic phase separation, we mainly review our own research.

3.1. Polymer solutions

3.1.1. Dilute polymer solutions: the moving droplet phase. Unusual behaviour of droplet phase separation was found in a dilute aqueous solution of poly(vinyl methyl ether), which has

a double-well-shaped phase diagram [28, 29]. It is unusual since after the formation of small droplets there is no coarsening. Droplets are moving vigorously by Brownian motion, but they rarely coalesce even if they collide with each other. This phase was named the *moving droplet phase* (MDP). For this particular mixture, this dynamic state is almost stable and persists for over a day [28]. Such behaviour can be explained if we regard droplets as elastic gel balls. It is induced only by a deep temperature jump and not by a shallow jump in the mixture. Thus, the strong dynamic asymmetry may be necessary for the appearance of the moving droplet phase. This phase may be in a 'dynamically stabilized state' and not in a thermodynamically stable state. Further studies are necessary to check the validity of such a concept.

To check the generality of this phenomenon, similar experiments were performed on a typical polymer solution composed of polystyrene (PS) and diethyl malonate (DEM) [30]. This mixture is known as an ideal polymer solution and the shape of the phase diagrams is well described by the standard theory of polymer solution. In this case, a moving droplet phase was also observed at low polymer concentrations, where droplets coarsen extremely slowly with time. The growth exponent is much less than the usual one ($\alpha = 1/3$) of the Brownian-coagulation mechanism and depends upon the quench depth. It was not so stable as in the case of PVME solutions, but the basic features were quite similar. This suggests that the appearance of a moving droplet phase may be universal for dilute polymer solutions for deep quenching (see section 9.1.4).

3.1.2. Solutions with near-critical compositions: phase inversion. A typical example of viscoelastic phase separation in a polymer solution [30] is shown in figure 3. Just after the temperature quench, the sample becomes cloudy; then after some incubation time (several seconds), small, but macroscopic solvent holes start to appear. This incubation period is called a 'frozen period' [30]. The number and the size of solvent holes increases with time (see figures 3(b) and 3(c)). The matrix-polymer-rich phase becomes networklike with the growth of solvent holes. The thin parts of the networklike structure are elongated and eventually broken

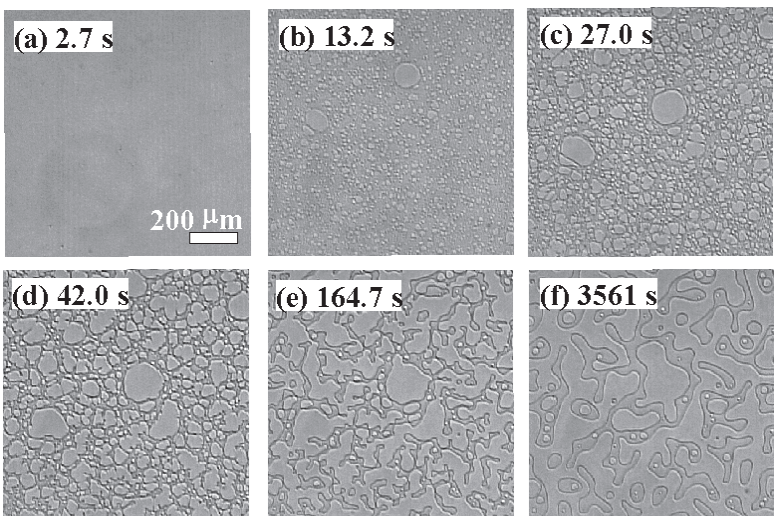

Figure 3. A phase-separation process observed with phase-contrast microscopy in a polymer solution of PS (molecular weight: 3.55×10^5) and diethyl malonate (6.78 wt% PS) at 9.3 °C, which is 7.2 K below the phase-separation temperature 16.5 °C. The number in each figure indicates a phase-separation time.

(see figures 3(d) and 3(e)). In this stage, the pattern is dominated by the *elastic force-balance* condition. In the final stage the networklike structure relaxes to a structure with a rounded shape and the domain shape starts to be dominated by the interface tension as in usual fluid–fluid phase separation (see figures 3(e) and 3(f)). It eventually becomes spherical droplets. During the period of figures 3(b)–3(e), the volume of the polymer-rich phase keeps decreasing with time and the contrast of that phase becomes more and more pronounced over time, reflecting the increase in the polymer composition of the polymer-rich phase. There occurs a clear phase inversion during phase separation. This phase inversion is a unique feature of viscoelastic phase separation.

Figure 4 shows the temporal change in the peak wavenumber q_{p} of the structure factor for two cases. The structure factor $S(q)$ was numerically calculated from a real-space image by two-dimensional Fourier transformation [55]. For the polymer solution of higher molecular weight the slope of the coarsening curve is smaller than for that of lower molecular weight. The time region of a steep decrease in q_{p} in the latter coincides well with that of a steep decrease in the volume of the PS-rich phase (see figure 5). This regime is called an 'elastic regime'. As described above, the coarsening behaviour is strongly dependent upon the molecular weights of PS and the quench depth. There is no universal feature in the coarsening behaviour. This is also confirmed by other experiments on mixtures of components with several different molecular weights under various quench conditions. However, there is a general feature that should be mentioned: with increase in the quench depth and the molecular weight of PS, the slope of q_{p} in the elastic regime decreases. It can also be noticed that q_{p} becomes constant for $t > t_{\mathrm{eh}}$, where $t_{\mathrm{eh}} \sim 100$ s corresponds to the timing of the crossover from an elastic to a hydrodynamic regime. Once a network structure transforms to a droplet structure, there are no fast coarsening mechanisms: neither the viscoelastic nor Siggia's hydrodynamic mechanism is active. We speculate that this slowing down of the coarsening may be related to the so-called 'pinning phenomenon' observed in polymer blends [15–17]. Finally, it should be stressed that the conventional analysis of the behaviour of $S(q)$ and q_{p} based on the scaling argument is almost meaningless for viscoelastic phase separation because of the absence of self-similarity.

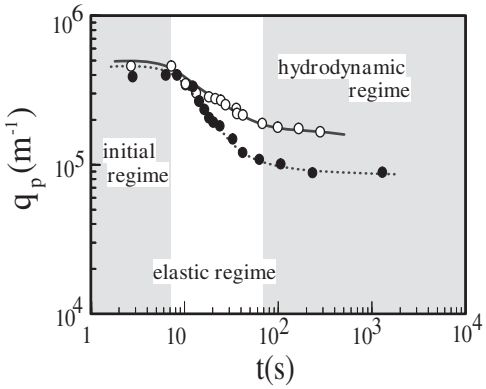

Figure 4. Temporal change in the peak wavenumber q_{p}. Open circles: for a mixture of PS (molecular weight: 3.55×10^5) and DEM (6.78 wt% PS) quenched at 9.3 °C (see figure 1); filled circles: for a mixture of PS (molecular weight: 1.90×10^5) and DEM (8.53 wt% PS) quenched at 0.0 °C (see figure 2). The solid and dashed lines are only to guide the eye.

Figure 5 shows the temporal changes in the area fraction of polymer-rich domains, Φ_{area}, and the number density of the solvent-rich droplets, n, which are obtained by a black-and-white operation of digital image analysis [55]. Φ_{area} steeply decreases with time in the intermediate

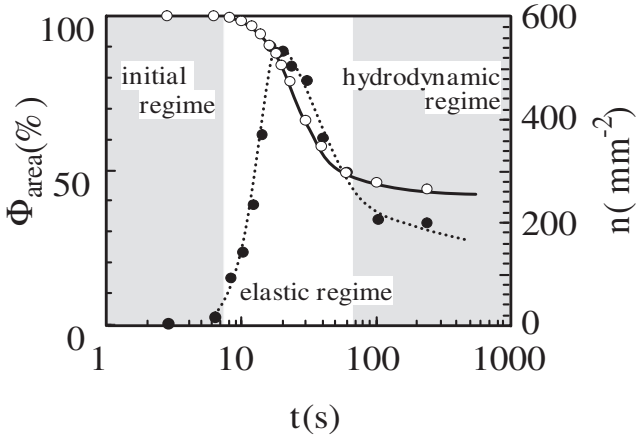

Figure 5. Temporal changes of Φ_{area} (open circles) and n (closed circles) in a polymer solution of PS (molecular weight: 1.90×10^5) and DEM (8.53 wt% PS) at 0.0 °C (see figure 2).

stage, in contrast to the common-sense expectation that after the formation of a sharp interface between the coexisting phase (namely, in the so-called late stage) the concentration of each phase will almost reach the final equilibrium one and, thus, there will be no change in the volume and concentration of each phase. As described in section 2, this is a key assumption behind the scaling theory of the late-stage domain coarsening. It was pointed out [30, 32] that the volume decrease of the more viscoelastic phase with time after the formation of a sharp interface is essentially the same as the volume shrinking of gels during volume phase transition [56–59]. The physical reason for this similarity to a gel will be discussed later. After several hundred seconds, the volume of each phase does not change so much and approaches the final equilibrium one determined from the equilibrium phase diagram.

The number density for the solvent-rich phase, on the other hand, initially increases with time, reflecting the nucleation of solvent-rich domains. Then it starts to decrease since the polymer-rich domains are stretched and broken by the large elastic deformation in the late stage (see figure 3). Finally, the number density of the solvent-rich droplets, n, should become 1/unit area in the very late stage since the solvent-rich phase becomes the matrix phase formed from the droplet phase because of 'phase inversion'.

3.1.3. The dynamic phase diagram. In figure 6 we show the phase diagram which summarizes what kind of phase separation is observed at a certain location in the phase diagram. We call it a 'dynamic phase diagram' [32]. In addition to the static composition symmetry, the dynamic symmetry between the two components of a mixture plays a crucial role in phase separation. A dynamic symmetry line (DSL) determines the threshold composition required for the formation of a percolated transient gel. There is also a transitional temperature region between the usual phase separation and viscoelastic phase separation. Below the transition temperature T_t, a transient gel is formed and phase separation is strongly modified by viscoelastic effects. However, this transition is not so sharp and is rather broad. The distance between the transition line T_t and the critical point T_c decreases with increase in the dynamic asymmetry. That is, it decreases with the degree of polymerization of the polymer N. In the limit of $N \to \infty$, $T_t \to T_\theta$ [32], where T_θ is the θ-temperature. Note that $\lim_{N\to\infty} T_c(N) = T_\theta$. This was recently confirmed experimentally for polymer solutions with very high molecular weights (the weight-average molecular weight $M_w > 10^6$). This leads to the conclusion that critical

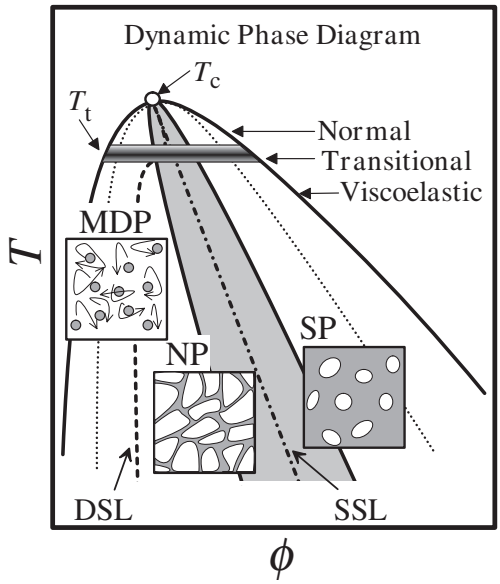

Figure 6. A schematic phase diagram including dynamic effects. Here both a static (composition) symmetry line (SSL) and a dynamic symmetry line (DSL) are drawn. The DSL is determined by whether a transient gel formed just after a quench is percolated or not. For shallow quenches we see normal phase separation, which can be explained by the static phase diagram (see figure 2). For deep quenches, we see viscoelastic spinodal decomposition: (i) the moving droplet phase (MDP) on the left of the DSL; (ii) networklike phase separation (NP) between the DSL and SSL, which is characterized by 'phase inversion'; and (iii) spongelike phase separation (SP) on the right of the SSL. In region (iii) near the SSL, a foamlike structure may be observed. For quenches with intermediate depths, there is a region of transition from normal to viscoelastic phase separation. The shaded region shows the statically nearly symmetric region, where a bicontinuous pattern may be observed.

phenomena and phase-separation phenomena in polymer solutions are essentially different from the conventional ones and strongly affected by the slow dynamics of polymers (see section 6.2.2). Please compare this phase diagram with the conventional one shown in figure 2.

3.2. Polymer mixtures only one of whose components has slow dynamics associated with the glass transition

Another example of viscoelastic phase separation [33] was observed in a mixture of PS and PVME, whose phase diagram is shown schematically in figure 7. This mixture is one of the most well-studied polymer mixtures as regards phase separation. Phase separation of this mixture has so far been believed to be typical of usual phase separation of binary liquid mixtures that is classified as described by a fluid model ('model H' in the Hohenberg–Halperin notation [4]). This is supported by many previous experiments [5, 6]. It may be true for a shallow temperature jump, for which the difference in the rheological property between the two phases is small because of the small difference in final concentration between them. It should be noted that for this mixture the difference in the degree of polymerization N itself is too small to cause dynamic asymmetry stemming from N-dependent molecular dynamics between the two coexisting phases. However, this polymer mixture can have strong dynamic asymmetry stemming from slow dynamics associated with glass-transition phenomena, especially for a deep temperature jump. The reasons are as follows:

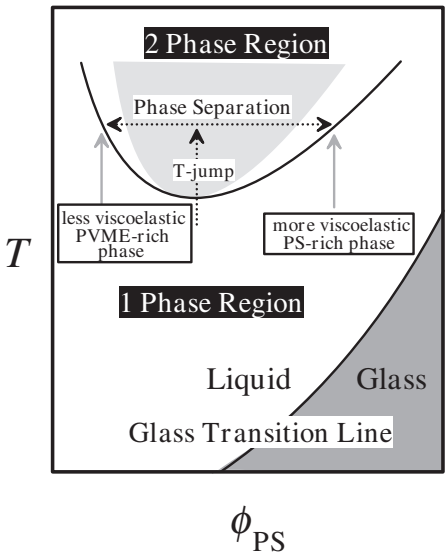

Figure 7. A schematic phase diagram of a mixture of PS and PVME. For a deep temperature jump, the strong dynamic asymmetry can be induced by the large difference in T_g between PS and PVME.

(1) The characteristic rheological time τ_t and the diffusion coefficient D of a phase with the composition of ϕ_{PS} are proportional to $\exp(-B/(T - T_g(\phi_{PS}))$ (B: constant; ϕ_{PS}: PS composition).

(2) $T_g(\phi_{PS})$ is strongly dependent upon ϕ_{PS} since T_g for PS ($T_g(1) \sim 100\ ^\circ$C) is very different from that for PVME ($T_g(0) \sim -26\ ^\circ$C).

Thus, τ_t for the PS-rich phase can be much longer than that for the PVME-rich phase (see figure 7) *for a deep temperature jump*, which causes the large composition difference between the two coexisting phases. This dynamic asymmetry can play a dominant role in the phase separation.

The phase-separation process of a mixture having the composition of 20 wt% PS is shown in figure 8. The system phase separates as a usual fluid mixture and becomes cloudy in the initial stage. Then, there is no significant coarsening for a certain period and, accordingly, no macroscopic domains are formed. As in the case of polymer solutions, this stage ($t \lesssim 800$ s) is called a 'frozen period'. After this frozen period, macroscopic holes (PVME-rich domains) appear and grow in size. Then, the PS-rich phase starts to shrink with time and the PS-rich phase transforms into a spongelike pattern. In the elastic regime ($\sim$800 s $< t \lesssim 2000$ s), the domain shape is determined by the mechanical balance of elastic forces and the interfacial tension plays few roles in determining the domain shape. That is, the elastic energy dominates the phase separation and the system behaves like an *elastic gel*. In the late stage of phase separation ($t \gtrsim 2000$ s), the system approaches its final equilibrium state; accordingly, the deformation rate of domains slows down, which leads to the weakening of the resulting stress fields. Thus, the PS-rich phase eventually behaves as a fluid and the domain shape transforms into the shape with the lowest interfacial energy (a sphere) as in usual phase separation. Since domains are isolated from each other, the coarsening rate is extremely slow after the disconnection of a networklike structure.

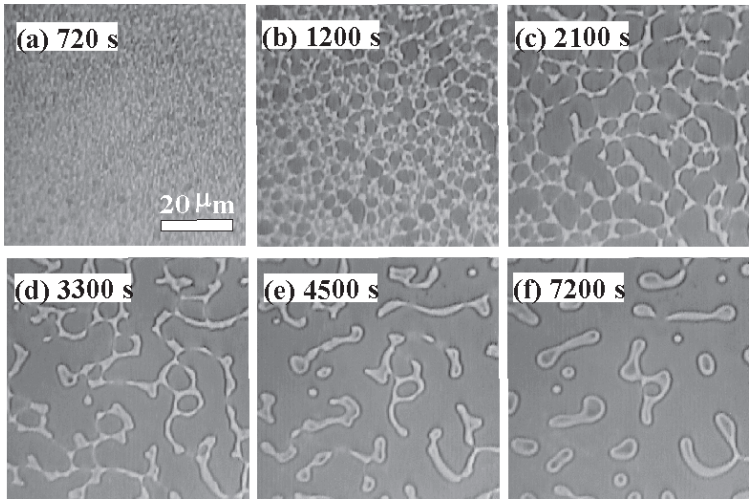

Figure 8. A pattern-evolution process in the phase separation of the PS-PVME mixture observed by video phase-contrast microscopy. The time shown in the figure is an elapsed time after the temperature jump.

Figure 9 shows a decrease in the area fraction Φ_{area} of the more viscoelastic (PS-rich) phase with time. This unusual behaviour is quite similar to that in figure 5. The phase-separation process can be divided into three regimes (see figure 9): the initial regime, the intermediate elastic regime and the final hydrodynamic regime. Only in the elastic regime does the volume fraction decrease steeply with time. Since the concentration must be conserved, this volume change tells us that the concentration of each phase changes with time by the transport (diffusion) of PVME from the PS-rich phase to the PVME-rich one through the phase boundary. This violates the well-accepted view of the late-stage phase separation that after the formation of a sharp interface the two phases are almost in equilibrium and the volume fraction is almost constant [1]. Since the absence of the concentration change after the

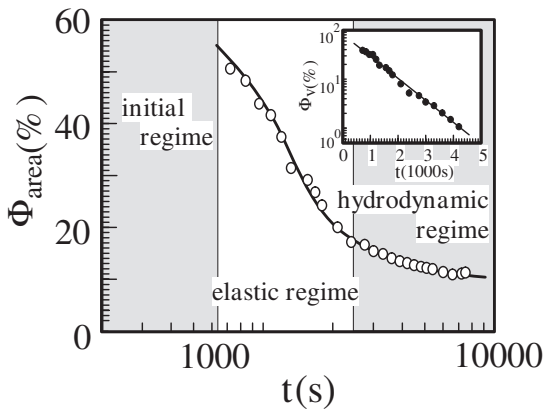

Figure 9. Temporal change in the apparent volume fraction (Φ_{area}) of the PS-rich phase. In the intermediate stage that we call an elastic gel-like regime, the volume fraction of the PS-rich phase steeply decreases with time. The small inset shows the semilog plot.

formation of a sharp interface is a prerequisite to self-similar growth, this result indicates that there is no self-similarity in pattern evolution for viscoelastic phase separation. This volume-shrinking process of the PS-rich phase should be essentially the same as the process of bulk phase separation in a gel, which itself has also remained largely unexplored so far [57–60].

We note that this mixture was recently studied also by Winter and co-workers [61] in detail and they observed a very similar pattern evolution. They measured rheological properties and NMR relaxation times in addition to morphological development. They demonstrated that a large network structure is composed of small network structures, by combining optical and electron microscopy. This suggests that the phase-separation pattern observed in a low magnification is a kind of 'coarse-grained' pattern. Thus, the composition change estimated from the macroscopic observation of the volume change of the phases might be apparent in the following sense. On the mesoscopic length scale, the local composition approaches the final equilibrium one in a rather early stage. The coarse-grained average composition in a macroscopic domain, however, changes very slowly even after the formation of an apparently sharp interface. It was also shown that rheological properties of a mixture are liquidlike in the one-phase region but that it behaves like gel in the network-forming regime of phase separation. The gel strength decreases with the phase-separation time. This is quite consistent with our picture of transient-gel formation just after the phase separation. Rather mild effects of dynamic asymmetry on the rheology of a polymer blend were also reported by Vlassopoulos *et al* [62].

3.3. Common features of and differences in pattern evolution between the above two systems

The pattern evolutions observed in the above polymer solution and polymer blend are essentially the same and there is no apparent qualitative difference between the two cases. This similarity suggests a universal nature of viscoelastic phase separation in dynamically asymmetric fluid mixtures, irrespective of the origin of the dynamic asymmetry [33]. As described later, however, there are some differences in the physical mechanism between them.

The characteristic feature of the pattern-evolution process is schematically summarized in figure 10 [32]. In the initial regime, usual growth of concentration fluctuations occurs. However, the viscoelastic effects soon start to prevent rapid growth of composition fluctuations characteristic of spinodal decomposition from proceeding further and the system becomes a frozen state (see figure 10(a)). Short-wavelength fluctuations produced in the initial stage are thus suppressed elastically. Then, the phase of slower dynamics becomes more and more viscoelastic with time and the system eventually behaves as an elastic body. Reflecting the transition from a viscous to an elastic state, the system changes the manner of phase separation from a fluid mode to a gel mode. Then, the less viscoelastic phase starts to appear as holes and these holes grow with time (see figure 10(b)). In the elastic regime (see figures 10(c) and 10(d)), the elastic force balance dominates the morphology instead of the interface tension, which leads to the anisotropic shape of the domain. Thus the matrix phase of slower dynamics forms a networklike structure. In the final stage (see figures 10(e) and 10(f)), the type of phase separation changes from gel-like to fluidlike, reflecting the slowing down of the phase separation. In this switching process stemming from the viscoelastic relaxation, the domain shape becomes spherical again since the interface energy overcomes the elastic energy. The spongelike structure becomes unstable in the absence of stress fields due to tube hydrodynamic instability [1, 46] and, thus, the interconnectivity breaks: a thickness difference along a tube of the slow-component-rich phase causes the internal pressure difference and produces a hydrodynamic flow. Thus, a thin part becomes thinner and eventually breaks, while a thick junction part becomes thicker and finally forms an isolated droplet. The shape relaxation from

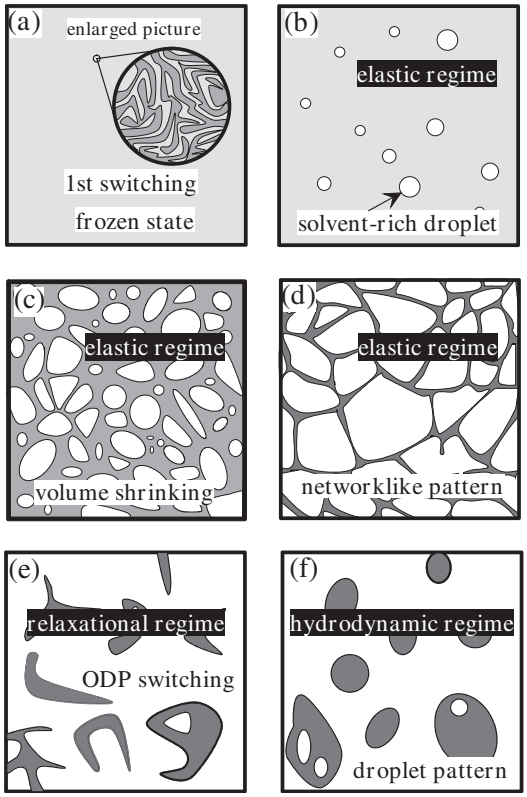

Figure 10. A schematic figure showing the characteristic features of the pattern evolution during viscoelastic phase separation of a mixture having a nearly critical composition.

a thin thread to a sphere is characterized by a time of $\eta R/\sigma$ (R: domain size; η: viscosity; σ: interface tension). The disruption of the network structure leads to a significant decrease in the coarsening rate, because only slow growth mechanisms such as evaporation–condensation and Brownian-coagulation mechanisms [1] can work for this isolated-domain morphology.

Finally we point out one obvious difference between polymer solutions and blends. In polymer solutions a moving droplet phase (MDP) exists, while in polymer blends it does not. Apparently, a low viscosity of the major phase is a prerequisite for the appearance of a MDP, or the dynamic stabilization of elastic droplets.

3.4. Absence of self-similarity

The most striking feature is the phase inversion during phase separation and the volume shrinking of the more viscoelastic (slow-component-rich) phase even after the formation of the sharp interface. The pattern-evolution process of a mixture of a nearly critical composition can be divided into three distinct regimes: the initial, intermediate and late stages. The transition between these regimes can be explained by 'viscoelastic relaxation in pattern evolution' and the resulting switching of the primary order parameter, as described later. This leads to the absence of self-similarity, which is well established in the late stage of 'usual' phase separation [1, 2]. The normalized structure factor $S(q/q_{\mathrm{p}})$ (q_{p}: a peak wavenumber of $S(q)$), for example, becomes broader with time, clearly indicating the absence of self-similarity. The

analysis of geometrical (topological) characteristics of domain patterns, such as mean and Gaussian curvatures and Euler number, clearly demonstrates the breakdown of self-similarity in a quantitative manner. Such analysis is particularly useful for a case where q_{p} apparently obeys the power law. It should be noted that the power-law behaviour is often apparently observed even in cases that lack self-similarity. The real-space analysis is much more useful for such a case [55, 63, 64]. The self-similarity relies on the existence of only one relevant length scale. Even in the linear regime or in the one-phase region, there are two length scales, the correlation length ξ and the viscoelastic length ξ_{ve} (see section 4.2 for its definition) for dynamically asymmetric mixtures. More important, the phase-separated pattern can never be characterized by one length scale under volume shrinking.

3.5. The concept of dynamic asymmetry

3.5.1. The physical origin of viscoelastic phase separation. The major common origin of viscoelastic phase separation described above is the 'dynamic asymmetry' between the components of a mixture. In all conventional theoretical models of phase separation, the two components of a mixture having the same dynamics (dynamic symmetry) is implicitly assumed, as reviewed in section 2. However, such an assumption is hardy valid for many mixtures because of the difference in the elementary dynamics between the components or the strong composition dependence of the mobility. Thus, it is a key to understanding the effects of dynamic asymmetry on phase separation and critical dynamics.

3.5.2. Possible origins of dynamic asymmetry. Here we consider various possible sources of dynamic asymmetry in condensed matter and point out various candidates for showing viscoelastic phase separation (see also section 10). Dynamic asymmetry may be caused by the size difference in component molecules of a mixture. Polymer solutions, colloidal suspensions, emulsions and protein solutions belong to this category. The effect of size difference is intrinsic and ideal viscoelastic phase separation may be observed. Dynamic asymmetry can also be caused by the existence of another transition, which induces slow dynamics. Such transitions include glass transition in usual liquids, spin-glass transition in magnetic systems and sol–gel transition in complex fluids. There are a number of studies on phase separation under the influence of glass transition [65–76] or gelation [77–86]. In this case, the relation between the phase diagram describing phase separation and a glass- or gel-transition line is quite important. Please refer to, e.g., reference [67], on interesting morphologies produced by phase separation under the influence of glass transition. Figure 11 schematically shows various possible types of phase diagram.

4. Theory

There are two different types of theoretical approach to introducing the dynamic asymmetry into a phase-separation model. One is based on a solid model, while the other is based on a fluid model.

4.1. A modified solid model

4.1.1. ϕ-dependent mobility. Dynamic asymmetry was effectively introduced in the solid model by assuming asymmetric ϕ-dependence of the kinetic coefficient $L(\phi)$ in the solid model (see equation (1)). This type of approach was first taken by Jäckle *et al* [73–76] in their studies on the effects of glass transition on phase separation (see figure 11(a)). They assumed

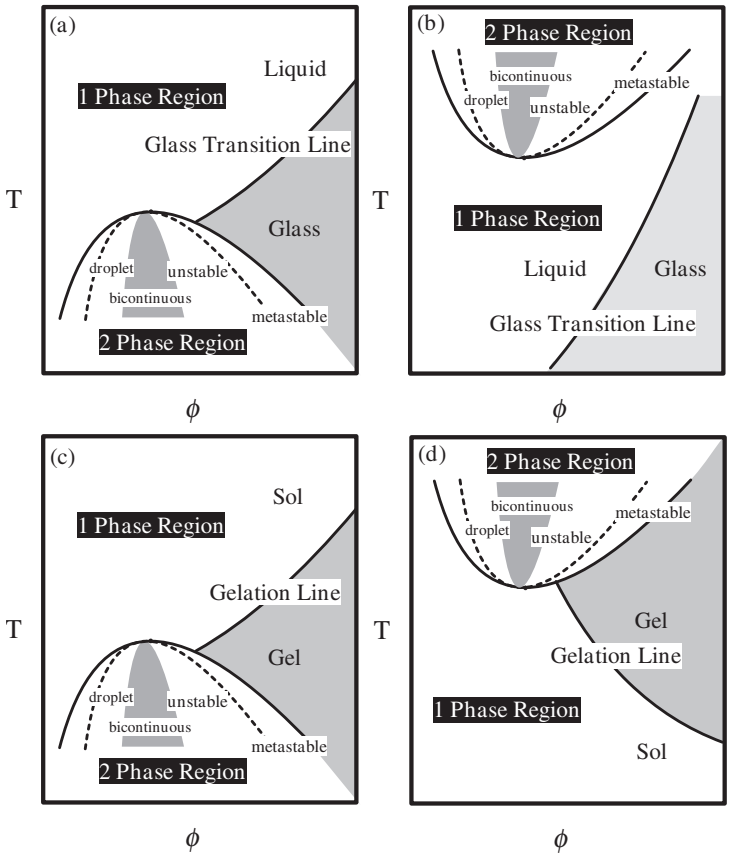

Figure 11. Various possible phase diagrams, in which phase separation can be affected by the dynamic asymmetry, which is induced by an additional transition. (a) A phase diagram of the upper-critical-solution-temperature (UCST) type with a glass-transition (or spin-glass-transition) line. (b) A phase diagram of the lower-critical-solution-temperature (LCST) type with a glass-transition line below it. (c) An UCST-type phase diagram with a sol–gel transition line. (d) A LCST-type phase diagram with a sol–gel transition line.

a strong ϕ-dependence of the diffusion constant, given as $D(\phi) = [\exp(\gamma(\phi - \phi_g) + 1]^{-1}$, where $\gamma > 0$. This relation with a large coefficient γ yields a rapid drop of D for $\phi > \phi_g$. This mimics the effects of glass transition. A similar approach was followed by Ahluwalia [87] and Vladimirova *et al* [88] in their simulation studies. However, it should be noted that there is no firm physical basis for the above functional form of $D(\phi)$. We also note that in this type of solid model viscoelastic stresses cannot play any roles in phase separation, simply because there are no velocity fields (see the discussion in section 5.3.3).

4.1.2. Introduction of an additional slow variable. Although we can include elastic effects in a solid model, it is not straightforward to include viscoelastic effects in a solid model since viscoelastic effects are intrinsic properties of liquids and not of solids in the exact sense. For very large η, however, a fluid model can be approximated by a solid model and it may be possible to 'formally' introduce a relaxational nature in a solid model by assuming the existence of an additional slow variable [89–91]. Using this type of approach the generalized

diffusion equation was derived by Binder, Frisch and Jäckle [65]. They assumed the existence of a slow variable and extended the functional derivative $\mu = \delta H/\delta\phi$ to a history-dependent one. The relaxational part of the chemical potential was expressed as

$$\delta\mu(\boldsymbol{q},t)|_{\rm rel} = \left[\left(\frac{\partial^2 f}{\partial\phi^2}\right)_{T,\infty} - \left(\frac{\partial^2 f}{\partial\phi^2}\right)_{T,0}\right]\int_{-\infty}^{t} {\rm d}t'\ \psi(t-t')\,\frac{\partial}{\partial t'}\,\delta\phi(\boldsymbol{q},t'). \tag{18}$$

Here the second derivatives of the free energy $(\partial^2 f/\partial\phi^2)_{T,\omega}$ for $\omega = \infty$ and $\omega = 0$ define the instantaneous and the quasi-static response of the chemical potential to a composition change. $\psi(\tau)$ is the relaxation function, which is normalized by the condition $\psi(0) = 1$ and decays to zero for $\tau \to \infty$. Thus, the total variation $\delta\mu(\boldsymbol{q},t)$ is obtained, up to linear order in $\delta\phi$, as

$$\delta\mu(\boldsymbol{q},t) = \delta\mu(\boldsymbol{q},t)|_{\rm rel} + \left[\left(\frac{\partial^2 f}{\partial\phi^2}\right)_{T,0} + Cq^2\right]\delta\phi(\boldsymbol{q},t). \tag{19}$$

By including a contribution $\Delta\mu(\boldsymbol{q},0)$ representing the deviations from local equilibrium just after the quench, which relaxes to zero as a relaxation function $\psi_1(t)$, the following generalized diffusion equation is obtained:

$$\frac{\partial}{\partial t}\,\delta\phi(\boldsymbol{q},t) + (D_0 + Kq^2)q^2\,\delta\phi(\boldsymbol{q},t) + Mq^2\,\Delta\mu(\boldsymbol{q},0)\,\psi(t) + [D_\infty - D_0]q^2\int_0^t {\rm d}t'\ \psi(t-t')\,\frac{\partial}{\partial t'}\,\delta\phi(\boldsymbol{q},t') = 0. \tag{20}$$

Here $D_\omega = M(\partial^2 f/\partial\phi^2)_{T,\omega}$ and $K = MC$ (M: mobility).

This pioneering approach is quite interesting, and the above equation is formally the same as the linearized dynamic equation of a viscoelastic model (see equation (56)). Thus, it can predict the essential features of the effects of a slow variable on the initial stage of phase separation. However, it should be noted that the introduction of a slow variable into a solid model is not so physically (or intuitively) easy to accept as the introduction of viscoelastic effects into a model of fluid mixtures. Thus, it may not be applied to our problem in a direct way. Further, its extension to the late-stage coarsening dynamics is not straightforward.

4.2. A two-fluid model

The dynamic coupling between stress and diffusion was first noticed by de Gennes and Brochard [92,93] when they considered the dynamics of concentration fluctuations in polymer solutions. The original form of the two-fluid model was derived from intuitive physical consideration. They introduced the concept of a viscoelastic length $\xi_{\rm ve}$. It is defined as $\xi_{\rm ve} \sim (D_\xi\tau_{\rm t})^{1/2}$ [93], where $\tau_{\rm t}$ is the characteristic time of the rheological relaxation and D_ξ is the diffusion constant. For the length scale longer than $\xi_{\rm ve}$, concentration fluctuations decay by diffusion, while for the length scale shorter than $\xi_{\rm ve}$, viscoelastic effects dominate [93]. The key idea of the two-fluid model is that we need two velocities, the polymer velocity and the solvent velocity, to properly describe (a) viscous drag effects and (b) the viscoelastic nature of the polymer chains. This idea was applied to the dynamics of gel [94] and polymer solutions [95].

Later, the two-fluid model was developed into a more formal theory. Helfand and Frederickson applied a dynamic coupling mechanism to sheared polymer solutions [96, 97]. Then, Onuki, Doi and Milner [98–101] developed a two-fluid model, which is a viscoelastic Ginzburg–Landau scheme with a conformation tensor as a new independent dynamic variable (see also references [102–104]). The two-fluid model was intensively studied in an effort to understand the so-called shear-induced phase separation found in polymer solutions [98–101,105,106]. The current form of the two-fluid model of polymer solutions and polymer

melts was derived by Doi [99], Doi and Onuki [100] and Milner [101]. The success of the two-fluid model in describing shear-induced phase separation was recently reviewed by Onuki [106] in detail.

Here we briefly review the derivation of the two-fluid model (see, e.g., references [92, 100, 101]). Let us consider a fluid mixture of components 1 and 2. Let $\boldsymbol{v}_1(\boldsymbol{r}, t)$ and $\boldsymbol{v}_2(\boldsymbol{r}, t)$ be the average velocities of components 1 and 2, respectively, and $\phi(\boldsymbol{r}, t)$ be the volume fraction of the component 1 at point $\boldsymbol{r}$ and time t. Here we assume that the two components have the same density ρ for simplicity. Then, the conservation law gives

$$\frac{\partial \phi}{\partial t} = -\boldsymbol{\nabla} \cdot (\phi \boldsymbol{v}_1) = \boldsymbol{\nabla} \cdot [(1-\phi)\boldsymbol{v}_2]. \tag{21}$$

The volume-average velocity v is given by

$$\boldsymbol{v} = \phi \boldsymbol{v}_1 + (1-\phi)\boldsymbol{v}_2. \tag{22}$$

The free energy of the system F_{mix} is given by

$$F_{\mathrm{mix}} = \int \mathrm{d}\boldsymbol{r} \left[f(\phi(\boldsymbol{r})) + \frac{C}{2} (\nabla \phi(\boldsymbol{r}))^2 \right] \tag{23}$$

where $f(\phi)$ is the free energy per unit volume of a mixture with the concentration ϕ of the component 1. The form of $f(\phi)$ depends upon the system; for example, it is given by the Flory–Huggins free energy [18] for polymer mixtures. Its time derivative can be written as

$$\begin{aligned} \dot{F}_{\mathrm{mix}} &= \int \left[\frac{\partial f}{\partial \phi} - C\,\nabla^2 \phi \right] \dot{\phi}\, \mathrm{d}\boldsymbol{r} = -\int \left[\frac{\partial f}{\partial \phi} - C\,\nabla^2 \phi \right] [\boldsymbol{\nabla} \cdot (\phi \boldsymbol{v}_1)]\, \mathrm{d}\boldsymbol{r} \\ &= \int (\boldsymbol{\nabla} \cdot \boldsymbol{\Pi}) \cdot \boldsymbol{v}_1\, \mathrm{d}\boldsymbol{r} \end{aligned} \tag{24}$$

where $\boldsymbol{\nabla} \cdot \boldsymbol{\Pi} = \phi\, \boldsymbol{\nabla}(\partial f / \partial \phi - C\,\nabla^2 \phi)$ and $\boldsymbol{\Pi}$ is the osmotic tensor. Here we also assume that the force $\boldsymbol{F}_i$ acts on the component i. Thus, the Rayleighian to be minimized is

$$R = \int \mathrm{d}\boldsymbol{r} \left[\frac{1}{2} \rho \frac{\partial}{\partial t} \boldsymbol{v}^2 + \frac{1}{2} \zeta(\phi)(\boldsymbol{v}_1 - \boldsymbol{v}_2)^2 + (\boldsymbol{\nabla} \cdot \boldsymbol{\Pi}) \cdot \boldsymbol{v}_1 - p \boldsymbol{\nabla} \cdot \boldsymbol{v} - \boldsymbol{v}_1 \cdot \boldsymbol{F}_1 - \boldsymbol{v}_2 \cdot \boldsymbol{F}_2 \right]. \tag{25}$$

In the above, the term containing the pressure p is added to guarantee that the incompressibility condition

$$\boldsymbol{\nabla} \cdot \boldsymbol{v} = 0. \tag{26}$$

is obeyed. The condition that the functional derivatives of the Rayleighian with respect to $\boldsymbol{v}_1$ and $\boldsymbol{v}_2$ be zero gives the following equations of motion:

$$\rho \frac{\partial (\phi \boldsymbol{v}_1)}{\partial t} = -\boldsymbol{\nabla} \cdot \boldsymbol{\Pi} - \zeta(\boldsymbol{v}_1 - \boldsymbol{v}_2) + \phi\, \boldsymbol{\nabla} p + \boldsymbol{F}_1 \tag{27}$$

$$\rho \frac{\partial [(1-\phi)\boldsymbol{v}_2]}{\partial t} = \zeta(\boldsymbol{v}_1 - \boldsymbol{v}_2) + (1-\phi)\, \boldsymbol{\nabla} p + \boldsymbol{F}_2. \tag{28}$$

Thus, the average velocity $\boldsymbol{v}$ obeys

$$\rho \frac{\partial \boldsymbol{v}}{\partial t} = -\boldsymbol{\nabla} \cdot \boldsymbol{\Pi} + \boldsymbol{\nabla} p + \boldsymbol{F}_1 + \boldsymbol{F}_2. \tag{29}$$

In the quasi-stationary condition, the velocity difference between the two components, on the other hand, obeys

$$\boldsymbol{v}_1 - \boldsymbol{v}_2 = -\frac{1}{\zeta} [(1-\phi)\boldsymbol{\nabla} \cdot \boldsymbol{\Pi} - (1-\phi)\boldsymbol{F}_1 + \phi \boldsymbol{F}_2]. \tag{30}$$

If $\boldsymbol{F}_i$ is expressed in terms of $\boldsymbol{v}_i$, the equations are closed and can be solved.

4.3. The viscoelastic model: coupling of phase separation with rheology

The above force $\boldsymbol{F}_i$ is determined by the rheological properties of a mixture. Thus, the phase-separation process is directly affected by the internal dynamics of the material itself. This causes a marked difference between viscoelastic phase separation and usual phase separation. Here we focus special attention on how the most general version of the viscoelastic model can be derived [34]. First we include the above-described concept of ϕ-dependent mobility in the solid model by introducing the ϕ-dependence of the friction constant $\zeta(\phi)$. The remaining task is to estimate the force acting on each component.

4.3.1. Origins of stress. To obtain the explicit form of the force $\boldsymbol{F}_i$, we need to understand how the stress is partitioned between the two components or to have the microscopic expression of the stress tensor of the material. The macroscopic total force $\boldsymbol{F}$ should be related to $\boldsymbol{F}_1$ and $\boldsymbol{F}_2$ as

$$\boldsymbol{F} = \boldsymbol{\nabla} \cdot \boldsymbol{\sigma} = \boldsymbol{F}_1 + \boldsymbol{F}_2. \tag{31}$$

Here $\boldsymbol{\sigma}$ is the total stress tensor, which is, in general, given by the constitutive equation of the material.

For simplicity, we assume Maxwell-type relaxation for both the shear and the bulk relaxation modulus, $G_j(\phi, t) = G_j(\phi)\exp(-t/\tau_j(\phi))$ (τ_j: the stress relaxation time). $j = \mathrm{S}$ stands for shear, while $j = \mathrm{B}$ stands for bulk. Here $G_j(\phi(\boldsymbol{r}))$ is the local elastic plateau modulus at $\boldsymbol{r}$ (after coarse-graining). $\boldsymbol{\sigma}$ is composed of the shear stress $\boldsymbol{\sigma}^{\mathrm{S}}$ and bulk stress $\boldsymbol{\sigma}^{\mathrm{B}}$ as $\boldsymbol{\sigma} = \boldsymbol{\sigma}^{\mathrm{S}} + \boldsymbol{\sigma}^{\mathrm{B}}$. Then $\boldsymbol{\sigma}^j$ obeys the following upper-convective Maxwell-type equation:

$$\frac{\partial \boldsymbol{\sigma}^j}{\partial t} + (\boldsymbol{v} \cdot \boldsymbol{\nabla})\boldsymbol{\sigma}^j = \boldsymbol{D} \cdot \boldsymbol{\sigma}^j + \boldsymbol{\sigma}^j \cdot \boldsymbol{D}^{\mathrm{T}} - \frac{\boldsymbol{\sigma}^j}{\tau_j(\phi)} + G_j(\phi)(\boldsymbol{D} + \boldsymbol{D}^{\mathrm{T}}) \tag{32}$$

where $\boldsymbol{D} = \boldsymbol{\nabla}\boldsymbol{v}_{\mathrm{r}}$ is the gradient tensor of $\boldsymbol{v}_{\mathrm{r}}$, which is the velocity relevant to the rheological deformation. Finally, we redefine $\boldsymbol{\sigma}^{\mathrm{S}}$ as

$$\boldsymbol{\sigma}^{\mathrm{S}} = \boldsymbol{\sigma}^{\mathrm{S}} - \frac{1}{d}\,\mathrm{Tr}(\boldsymbol{\sigma}^{\mathrm{S}})\boldsymbol{I}$$

while we redefine $\boldsymbol{\sigma}^{\mathrm{B}}$ as

$$\boldsymbol{\sigma}^{\mathrm{B}} = \frac{1}{d}\,\mathrm{Tr}(\boldsymbol{\sigma}^{\mathrm{B}})\boldsymbol{I}.$$

If we neglect the translation and rotation of the stress tensor, $\boldsymbol{\sigma}$, it reduces to the most general expression for σ_{ij} in the linear theory of elasticity [107]:

$$\sigma_{ij} = \int_{-\infty}^{t} \mathrm{d}t' \,[G_{\mathrm{S}}(t - t')\kappa_{\mathrm{r}}^{ij}(t') + G_{\mathrm{B}}(t - t')(\boldsymbol{\nabla} \cdot \boldsymbol{v}_{\mathrm{r}}(t'))\delta_{ij}] \tag{33}$$

where

$$\kappa_{\mathrm{r}}^{ij} = \frac{\partial v_{\mathrm{r}}^j}{\partial x_i} + \frac{\partial v_{\mathrm{r}}^i}{\partial x_j} - \frac{2}{d}(\boldsymbol{\nabla} \cdot \boldsymbol{v}_{\mathrm{r}})\delta_{ij}. \tag{34}$$

$G_{\mathrm{S}}(t)$ and $G_{\mathrm{B}}(t)$ are material functions, which are called the shear and bulk relaxation modulus, respectively. Here it should be noted that $G_{\mathrm{B}}(t)$ does not contain the bulk osmotic modulus, $K_{\mathrm{os}} = \phi^2(\partial^2 f/\partial\phi^2)$. We have the relation $\eta = \int_0^\infty G_{\mathrm{S}}(t)\,\mathrm{d}t$, where η is the viscosity of the material.

The second term of equation (33) was introduced to incorporate the effect of 'effective' volume change into the stress tensor [34, 108]. In a two-component mixture, the mode associated with $\boldsymbol{\nabla} \cdot \boldsymbol{v}_{\mathrm{r}}$ can exist as long as $\boldsymbol{v}_{\mathrm{r}} \neq \boldsymbol{v}$, even if the system is incompressible. It should

be stressed that its diagonal nature leads to the direct coupling with diffusion: note that the effective osmotic pressure is given by

$$\pi^{\rm eff} = \left(\phi\frac{\partial f}{\partial \phi} - f\right) - \int_{-\infty}^{t} {\rm d}t'\, G_{\rm B}(t-t')\boldsymbol{\nabla}\cdot\boldsymbol{v}_{\rm r}(t').$$

It should be noted that this term is important even in the case of polymer solutions, as described later, although this term has so far been ignored (or, more strictly, not treated as an important physical factor) in the previous theories [99–101, 109]. This is partly because it may not be important in the problem of shear-induced phase separation [106] and such a bulk modulus does not play any important role in rheology for polymers in good or θ-solvents, namely, in the equilibrium state [18, 19, 100]. Note that there are few dynamic theories of polymers in poor solvents. We stress that the interaction network (or transient gel) and the associated bulk and shear modulus are key physical factors for understanding 'viscoelastic phase separation' [34, 108], as will be described in section 5.

4.3.2. Asymmetric stress division: stress division parameter α_k and force $\boldsymbol{F}_k$. Here we consider the physical meaning of $\boldsymbol{v}_{\rm r}$. In a linear response regime, the rheological velocity $\boldsymbol{v}_{\rm r}$ is generally given by a linear combination of $\boldsymbol{v}_1$ and $\boldsymbol{v}_2$ [100, 109]:

$$\boldsymbol{v}_{\rm r} = \alpha_1\boldsymbol{v}_1 + \alpha_2\boldsymbol{v}_2. \tag{35}$$

Then, the next problem is that of how the stress is partitioned between the two components. Since $\boldsymbol{F}\cdot\boldsymbol{v}_{\rm r}$ should be equal to $\boldsymbol{F}_1\cdot\boldsymbol{v}_1 + \boldsymbol{F}_2\cdot\boldsymbol{v}_2$ in the Rayleighian, we have the following stress division:

$$\boldsymbol{F}_1 = \alpha_1\boldsymbol{F} \qquad \boldsymbol{F}_2 = \alpha_2\boldsymbol{F} \tag{36}$$

where $\alpha_1 + \alpha_2 = 1$ from equation (31).

Here we consider the physical meaning of the forces $\boldsymbol{F}_k$ more explicitly [34]. The forces acting on the component k are (i) the friction between the component k and the other component due to their relative motion and (ii) the rheological coupling between the component k and the surrounding rheological environment made of the component k itself. This can be easily understood by considering a gel that is composed of a polymer network and a solvent, as an example: the motion of the polymer is affected by the two forces, namely, the friction force against the solvent (viscous drag effects) and the elastic force due to the network deformation. Thus, it is natural to think that $\boldsymbol{F}_k$ ($k = 1, 2$) corresponds to a force of type (ii), namely, the force acting on the component k due to the motion of the component k ($\boldsymbol{v}_k$) itself and not due to that of the other component. Thus, we assume that $\boldsymbol{F}_k$ is linear in $\boldsymbol{v}_k$:

$$\boldsymbol{F}_k = \boldsymbol{\nabla}\cdot\boldsymbol{\sigma}^{(k)} \tag{37}$$

$$\sigma_{ij}^{(k)} = \int_{-\infty}^{t} {\rm d}t'\,[G_{\rm S}^{(k)}(t-t')\kappa_k^{ij}(t') + G_{\rm B}^{(k)}(t-t')(\boldsymbol{\nabla}\cdot\boldsymbol{v}_k(t'))\delta_{ij}] \tag{38}$$

where

$$\kappa_k^{ij} = \frac{\partial v_k^j}{\partial x_i} + \frac{\partial v_k^i}{\partial x_j} - \frac{2}{d}(\boldsymbol{\nabla}\cdot\boldsymbol{v}_k)\delta_{ij}. \tag{39}$$

Here the unknown factors are the functional shapes of $G_{\rm S}^{(k)}(t)$ and $G_{\rm B}^{(k)}(t)$ for the motion of the component k, instead of α_k.

4.4. Basic equations of a viscoelastic model

Here we summarize the basic equations describing a viscoelastic model:

$$\frac{\partial \phi}{\partial t} = -\boldsymbol{\nabla} \cdot (\phi \boldsymbol{v}) - \boldsymbol{\nabla} \cdot [\phi(1-\phi)(\boldsymbol{v}_1 - \boldsymbol{v}_2)] \tag{40}$$

$$\boldsymbol{v}_1 - \boldsymbol{v}_2 = -\frac{1-\phi}{\zeta}\left[\boldsymbol{\nabla} \cdot \boldsymbol{\Pi} - \boldsymbol{\nabla} \cdot \boldsymbol{\sigma}^{(1)} + \frac{\phi}{1-\phi}\boldsymbol{\nabla} \cdot \boldsymbol{\sigma}^{(2)}\right] \tag{41}$$

$$\rho \frac{\partial \boldsymbol{v}}{\partial t} \cong -\boldsymbol{\nabla} \cdot \boldsymbol{\Pi} + \boldsymbol{\nabla} p + \boldsymbol{\nabla} \cdot \boldsymbol{\sigma}^{(1)} + \boldsymbol{\nabla} \cdot \boldsymbol{\sigma}^{(2)}. \tag{42}$$

We also need equation (22), equation (26) and equation (32) or (38) as the basic equations. Here it should be noted that we need the phenomenological or microscopic theories describing the forms of $G_{\mathrm{S}}(t)$ and $G_{\mathrm{B}}(t)$ or those of $G_{\mathrm{S}}^{(k)}$ and $G_{\mathrm{B}}^{(k)}$. Since the above basic equations are derived relying solely upon a two-fluid model, they should be independent of the types of material and quite general.

5. The interaction network (transient gel) and asymmetric stress division

Let us first focus on some specific problems to obtain a deeper insight into the origins of stress and how the resulting stress is partitioned between the two components of a mixture. We propose to group viscoelastic phase separation into two types, type A and B, in terms of the origin of the dynamic asymmetry. Type A may be unique to a mixture of large size asymmetry, which is composed of large molecules (or large particles) and a 'simple liquid'. In this type, only the slow component can support elastic stress, while the fast (liquid) component cannot. In other words, perfect stress division is expected. In type B, on the other hand, the stress division is asymmetric, but both components can support stress. Type B is common to mixtures having strong ϕ-dependent mobility. It should be noted here that a moving droplet phase (MDP) exists only in type-A mixtures. We also consider some general features of asymmetric stress division.

5.1. Type A: perfect stress division, the interaction network and transient gel

In type A, dynamic asymmetry is intrinsically induced by a large difference in size of the component molecules. For example, complex fluids such as polymer solutions, colloidal suspensions, emulsions, micellar solutions and protein solutions belong to type A. A system of type A is characterized by the fact that the elementary dynamics of the fast component is much faster than the characteristic deformation rate of phase separation and it always behaves as 'fluid'. In other words, the interaction network of the fast component relaxes to its lower energy state (a compact structure) quite rapidly. We consider the asymmetric stress division in type A for a few examples. Since the perfect stress division is realized in type A, we can set $\boldsymbol{v}_{\mathrm{r}} = \boldsymbol{v}_1$, supposing component 1 to be the slow component.

5.1.1. Polymer solutions. First we point out an obvious, but important fact. Phase separation of the polymer solution always occurs in a poor solvent. Thus, polymer dynamics in a poor solvent is a key to understanding critical phenomena and phase-separation phenomena. Unfortunately, however, there are no established theories that describe polymer dynamics in a poor solvent. In a poor solvent, we need to seriously consider attractive interactions between polymer chains in addition to topological interactions, which play a dominant role in polymers in theta and good solvents [18, 19]. The most natural model may be a transient-gel

model [34, 108], where the transient gel is induced by the interpolymer attractive interactions between polymer chains. It is worth mentioning that such a transient gel is stabilized by the driving force of phase separation itself. For polymer solutions, we can speculate on a few different scenarios:

(i) Just after a temperature quench a coil–globule transition takes place in individual polymers. A globule may be composed of parts of more than two chains. In this case, the junction point of a transient gel may be a globule.
(ii) If a globule is isolated initially, on the other hand, the situation is very similar to the transient-gel formation in colloidal suspensions.
(iii) The other extreme is a gel similar to chemically crosslinked gel. In this case, any parts of chains form a junction point.

We think that cases (i) and (ii) are probable. Since the situation is selected kinetically, however, it may be dependent upon the molecular weight and concentration of polymers. For example, case (ii) may be the case for dilute polymer solutions near the DSL (see figure 6). Provided that the formation of a transient gel is a generic feature of polymers in a poor solvent, we can expect $G_{\mathrm{B}}^{(1)}(t)$ to play an important role in viscoelastic phase separation [34]: the transient network of topological origin itself (entanglement effects) does not lead to the bulk relaxation mode [19], while the transient network formed by attractive interactions does clearly make the bulk relaxation mode active. It may be this mode that is primarily responsible for the volume-shrinking behaviour of a more viscoelastic phase observed in the experiments [29, 30, 33].

Further theoretical studies on the formation of a transient gel in poor solvents [110], its rheological properties [111, 112] and its temporal change during phase separation [113] are highly desirable. Microscopic simulations would be useful for understanding the kinetics of the formation of a transient gel. Experimentally, a cryo-TEM method [114] may be useful to reveal the structure of a transient gel.

5.1.2. Colloidal suspensions, emulsions and protein solutions. Recently it was found [115–118] that the addition of non-absorbing polymers to a colloidal suspension causes phase separation. This is due to polymer-induced depletion attraction between colloidal particles [119]. When colloids are close enough, there is an overlap of the depletion zone from which polymers are sterically excluded. The resulting unbalanced osmotic force causes attractive interactions between colloidal particles.

Depending upon the sizes of polymers and colloids and their compositions, a variety of phase-separation behaviours are observed [120–125], including (i) fluid–fluid phase separation, (ii) gel-like phase separation and (iii) phase-separation-induced crystallization. For example, when colloidal suspensions are brought shallowly into an unstable region (case (i)), the early stage of phase separation cannot be described by the standard Cahn linear theory and the transport coefficient apparently has a strong q-dependence [121, 122]. For a deep quench (case (ii)), on the other hand, the initial growth of the concentration fluctuations is followed by the formation of a transient gel, and the coarsening process apparently stops for a while. This transient-gel state persists for a long time, and then the gel eventually collapses under gravity [120–124]. Three-dimensional microscopic observation reveals that big holes are slowly created in a transient gel during the above process [122–124]. Its final state can be well described by the thermodynamic phase diagram. The initial stage of the aggregation process was also studied by Brownian dynamics simulations [126–130]. Further, quite similar phenomena are observed in phase separation of other types of colloidal suspensions [131] and also that of emulsions [132, 133]. In micellar casein–galactomannan mixtures, Bourriot *et al* found that the phase-separation process yields a continuous network mostly composed

of the aggregated micellar casein, which results in viscoelastic evolution in the two-phase region [134]. The essential features of these unusual phase-separation behaviours in colloidal suspensions and emulsions may also be well described by the viscoelastic model [135].

Colloidal suspensions and polymer solutions are similar in the sense that both are two-component liquids with large size difference between the components. Thus, they have intrinsic 'dynamic asymmetry' between their components. This feature leads to their interesting rheological properties including the strong composition dependence of the viscosity, η. Despite their similarity, however, their fields have developed rather independently, partly because they are topologically quite different. This topological difference leads to the difference in the type of particle or molecular motion. More important, polymers have large numbers of internal degrees of freedom, while colloids do not. The large numbers of internal degrees of freedom allow even individual polymer chains to bear mechanical stress under strain fields. This can give rise to asymmetric stress division. In contrast, individual colloidal particles cannot bear any stress because they are 'rigid' particles (soft gel particles are exceptional). This difference makes colloidal gels much more fragile than polymer gels, which may cause crucial differences in their non-linear rheology. Thus, one may think that it is not so obvious whether phase separation of colloidal suspensions can be explained by the same viscoelastic mechanism as that which is operative in polymer solutions. Paradoxically, colloidal suspension is an ideal system to consider when investigating the role of the 'interaction network' and its relation to viscoelastic phase separation.

It was recently proposed [135] that the interaction network of colloidal particles can bear mechanical stress via topological and energetic interactions, even though individual particles cannot. In a two-phase region, attractive interactions between like species prevail over the entropic driving force of mixing. Thus, components having a larger size (colloids) form their own interaction network. An important point is that its characteristic relaxation time is much slower than that of the liquid component having a smaller size. This is the origin of strongly asymmetric stress division. The dynamic phase diagram of colloidal suspensions may basically be the same as the dynamic phase diagram of polymer solutions (see figure 6). On the basis of this idea, we schematically explain in figure 12 how the manner of phase separation depends upon the initial composition and the quench depth. In the figure, T^{e} is the effective temperature, which is a function of polymer concentration that is added to induce the depletion force. If a system is brought into a transient-gel region from a one-phase region, the plateau modulus of a system changes drastically from $G(\phi)$ to $G_{\mathrm{tg}}(\phi)$, as shown in figure 12, reflecting the formation of a transient gel. This picture is supported by direct rheological measurements of phase-separating emulsions [133, 134]. It may explain the transition from apparently ordinary fluid–fluid phase separation to a transient-gel behaviour at around $T^{\mathrm{e}}_{\mathrm{tg}}$ [120–124].

5.1.3. Common features of polymer solutions and colloidal suspensions: transient-gel formation. The most striking feature common to polymer solutions and colloidal suspensions is the formation of a transient gel in the initial stage of phase separation. It is the most unique feature of viscoelastic phase separation. A transient gel represents the direct appearance of the 'interaction network', which originates from strong attractive interactions between like species that may universally exist in the two-phase region of a dynamically asymmetric mixture. In fact, it was 'commonly' observed in phase separation of polymer solutions [30], polymer blends [33, 61], colloidal suspensions [120–124] and emulsions [133, 134]. Thus, *the appearance of a transient gel should be quite universal for phase separation of dynamically asymmetric mixtures* [34, 135].

In polymer solutions, the rheological relaxation time τ was conventionally believed to be the reptation time for purely topological interactions [97, 100, 101, 105, 106, 151]. However, it

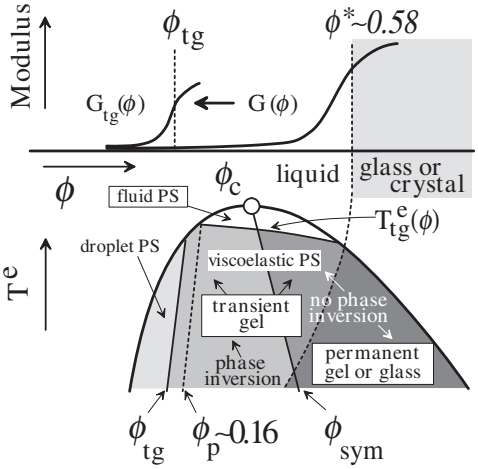

Figure 12. Schematic figures showing the equilibrium and transient modulus (upper figure) and the corresponding dynamic phase diagram of a colloidal suspension (lower figure) predicted by our model. PS stands for phase separation. Φ_{tg} corresponds to the DSL in the dynamic phase diagram of a polymer solution. The upper figure represents a rapid change in the mechanical properties of a mixture, which is induced by the formation of a transient gel after a deep quench.

was recently demonstrated [34, 108] that this should be the relaxation time of the interaction network of polymers (or a transient gel) itself under poor-solvent conditions. Similarly, the slow dynamics of colloidal suspensions should have both topological and *energetic* origins. Although colloidal particles have no internal degrees of freedom, in contrast to polymers, the motion of particles is affected by both topological trapping (cage effects) and energetic trapping due to attractive interactions. In colloidal phase separation, thus, τ should also be the characteristic relaxation time of the interaction network itself (a transient gel for a deep quench) [135].

For colloid phase separation, a particle network initially has a rather open, or tenuous, structure because of the random sticking process of particles under long-range hydrodynamic interactions, and then slowly becomes more compact, or more dense, to lower the free energy (see figure 13). Note that compact aggregates are characterized by a large number of nearest neighbours. This change of particle configuration in colloidal suspensions corresponds to a transition from a transient-gel state to the final equilibrium state in viscoelastic phase separation of polymer solutions. This picture is confirmed by our recent numerical simulations of phase separation of colloidal suspensions [136]. A similar picture may basically be applied to polymer solutions.

5.2. Type B: ϕ-dependent mobility and transient gel

For type B, dynamic asymmetry is induced by both the strong ϕ-dependence of the mobility or friction constant $\zeta(\phi)$ and the formation of the interaction network. Here we consider two examples, a mixture of polymers having different chain lengths (N) and a mixture of molecules having very different values of T_g.

5.2.1. Polymer mixtures. In the case of a mixture of polymers 1 and 2, whose degrees of polymerization are N_1 and N_2, respectively, the stress produced by the motion of polymer 1 can be different from that produced by the motion of polymer 2. Intuitively, the motion of a

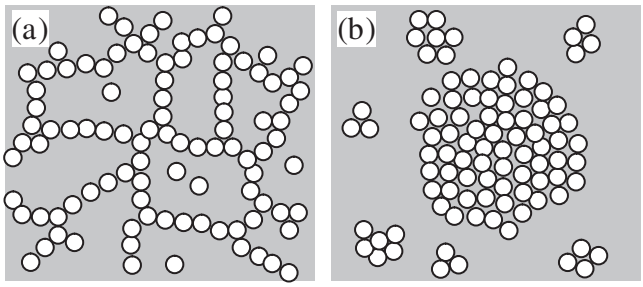

Figure 13. The change in the particle configuration from an open tenuous (a) to a compact structure (b) for colloidal suspensions. An open structure corresponds to a transient gel. A transient-gel state is in a higher energy state and the system tries to lower the energy by increasing the number of the nearest neighbours. Mechanical stress originating from interparticle attractive interactions stretches the arms of a transient gel and leads to their break-up. In this way, an open structure relaxes to a lower-energy structure, namely, a compact structure.

longer chain causes stronger stress than that of a shorter chain. Following the Brochard theory on mutual polymer diffusion [137], which is based on the reptation theory that deals only with the effect of topological constraints (tube) on entangled polymer chains, Doi and Onuki [100] explained how the stress should be divided between the two polymers with different lengths. According to them,

$$\boldsymbol{v}_{\mathrm{r}} = \boldsymbol{v}_{\mathrm{T}} = \alpha_1 \boldsymbol{v}_1 + \alpha_2 \boldsymbol{v}_2 \tag{43}$$

$$\alpha_k = \frac{\zeta_k}{\zeta_1 + \zeta_2} = \frac{\phi_k N_k}{\phi_1 N_1 + \phi_2 N_2} \tag{44}$$

where $\boldsymbol{v}_{\mathrm{T}}$ is the tube velocity. Here ζ_k is the friction of the component k with the tube surrounding it. ζ_k is given by $\zeta_k = \phi_k(N_k\zeta_0/N_{\mathrm{e}})$ [100], where ϕ_k is the volume fraction of the component k, ζ_0 is the microscopic friction constant and N_{e} is the average degree of polymerization between the entanglement points. The resulting stress division is given by $\boldsymbol{F}_k = \alpha_k \boldsymbol{\nabla} \cdot \boldsymbol{\sigma}$ [100]. Here it should be stressed that ζ_k is the crucial quantity in the sense that it represents the strength of the coupling between the component k (the volume fraction of ϕ_k) and the surrounding rheological environment (a tube in this case).

It should be noted here that the above stress division parameter is determined solely from the topological consideration. The energetic factors are completely excluded from consideration. Note that near to and below a critical point T_{c}, we always have to consider the role of the attractive interactions between the same kinds of polymer. This increases the rheological coupling, namely, ζ_k and, more important, leads to the formation of a transient gel. The inclusion of energetic interactions is a prerequisite to the description of polymer dynamics during phase separation [34].

5.2.2. A mixture of components having very different glass-transition temperatures (T_g). In this case, we also expect an asymmetric stress division since the two kinds of component molecule are expected to feel the rheological environment very differently, as in the case of polymer mixtures, even if the mean-field rheological environment surrounding them is the same. It is easy to imagine that a high-T_{g} component has less friction with the local rheological environment than a low-T_{g} component does. Recent theoretical studies on supercooled binary liquids [138] based on the mode-coupling approximation support such a picture. If we introduce formally the coupling strength ζ_k for the component k that is proportional to ϕ_k, the stress division can be expressed by the same relation as that for polymer mixtures. The mean-field

rheological environment in this problem of glass transition is the so-called 'cage' [139, 140]. *The concept of a 'cage' in glass transition is quite similar to the concept of a 'tube' in polymer mixtures.* The time for escape of a molecule from a 'cage' or 'tube' gives the relaxation time of $G(t)$ in both cases. Unfortunately, we do not have a reliable theoretical basis even for a simple liquid–glass transition; and, thus, it is difficult to obtain specific quantitative expressions for ζ_k at present. Phenomenologically, however, it is known that $G(t) = G_0 \exp[-(t/\tau)^\beta]$ and $\tau \sim \tau_0 \exp(B/(T - T_0))$, where β is the stretching parameter ($0 \leqslant \beta \leqslant 1$) and T_0 is the so-called Vogel–Fulcher temperature.

It should be stressed again that we have to take into account the effects of attractive interactions between the same species on their dynamics below T_c [34].

5.3. The physical origin of the asymmetric stress division: the concept of an interaction network

Here we consider the problem of what is the most basic physical factor responsible for asymmetric stress division, on the basis of intermolecular or interparticle interactions. The network of attractive interaction is universally formed when a mixture is quenched into its metastable or unstable state since there effectively exist attractive interactions between the same components. In dynamically symmetric mixtures, the interaction network always relaxes into its equilibrium state in a time much shorter than the phase-separation time. In dynamically asymmetric mixtures, however, the relaxation times of the interaction network are different for the two components because of the mobility (or size) difference, and that of a slow component can be longer than the characteristic time of phase separation.

5.3.1. A general rule for stress division. First we discuss a general rule for the stress division in viscoelastic matter. We already obtained the general relation given by (equation (35)) $\boldsymbol{v}_r = \alpha_1 \boldsymbol{v}_1 + \alpha_2 \boldsymbol{v}_2$, with $\alpha_1 + \alpha_2 = 1$. For the motion of the component k having the velocity of $\boldsymbol{v}_k$ relative to the mean-field rheological environment having the velocity of $\boldsymbol{v}_r$, the friction force is given by $\zeta_k(\boldsymbol{v}_r - \boldsymbol{v}_k)$, where ζ_k is the average friction of the component k and the mean-field rheological environment at point $\boldsymbol{r}$, where the volume fraction of the k-component is $\phi_k(\boldsymbol{r})$. Here $\zeta_k = \phi_k \zeta_k^m$ and ζ_k^m is proportional to the friction between an individual molecule of the component k and the mean-field rheological environment, which we call the generalized friction parameter. From the physical definition of the mean-field rheological environment, the two friction forces should be balanced. This fact guarantees that the rheological properties can be described using just $\boldsymbol{v}_r$ as in equation (33). Thus, we have the following relation, in general:

$$\zeta_1(\boldsymbol{v}_r - \boldsymbol{v}_1) + \zeta_2(\boldsymbol{v}_r - \boldsymbol{v}_2) = 0. \tag{45}$$

From equations (35) and (45), we obtain the general expression for the stress division parameter α_k:

$$\alpha_k = \frac{\phi_k \zeta_k^m}{\phi_1 \zeta_1^m + \phi_2 \zeta_2^m}. \tag{46}$$

The above relation is consistent with a simple physical picture in which the friction is just the origin of the coupling between the motion of the component molecules and the rheological medium. The above relation is a natural extension of the stress division in polymer mixtures [100], where $\boldsymbol{v}_r$ is the tube velocity $\boldsymbol{v}_T$. We expect this relation to hold, irrespective of the microscopic details of rheological models. For type-A mixtures, $\zeta_1 \gg \zeta_2$, and thus we obtain $\boldsymbol{v}_r \cong \boldsymbol{v}_1$. To be more exact, equation (38) is useful for such a case of an extremely asymmetric stress division.

5.3.2. Transient gel. Next we need to consider the rheological functions, which are coupled with the deformation rate expressed by using v_r. Focusing on the formation of a transient gel, we consider the origin of the bulk stress, using colloidal suspensions as an example. The bulk stress has not been considered to be important in conventional problems. However, it plays a key role in viscoelastic phase separation [34, 108]. Since colloidal particles do not have internal degrees of freedom, they do not have any viscoelastic properties. Intuitively, it may be difficult to accept the significance of viscoelastic effects in colloidal suspensions. Thus, it can be a good example to illustrate the physical origin of the bulk stress.

Figure 14 schematically shows the situation of a transient gel formed in a colloidal suspension. When we try to reduce or increase the effective volume over which some colloidal particles forming the interaction network spread, by using a membrane through which only liquid molecules can pass and colloids cannot, the membrane should feel not only the osmotic pressure but also the bulk mechanical stress, when it moves faster than the characteristic relaxation rate, $1/\tau_B$. This originates from the 'elasticity of the network' or the 'topological constraint for diffusion'; that is, the network tries to move while retaining the 'connectivity'. It is easy to see that this process, which is characterized by τ_B, would be very slow.

Before discussing the situation in a two-phase region, it is worth noting the difference in longitudinal viscosity between polymer solutions and colloidal suspensions in a one-phase region. The reptation theory [19] tells us that the bulk stress originating from polymers decays very quickly in polymer solutions under 'good-solvent' conditions. Thus, we need not consider the bulk stress coming from polymers, as long as we consider slow dynamics in a good solvent. For colloidal particles, it is known that there can exist longitudinal viscosity even for a homogeneous system in a one-phase region [141–143]. This originates from the 'topological constraint' via repulsive interactions and/or long-range hydrodynamic interactions.

Here we consider both the similarity of and essential differences among permanent

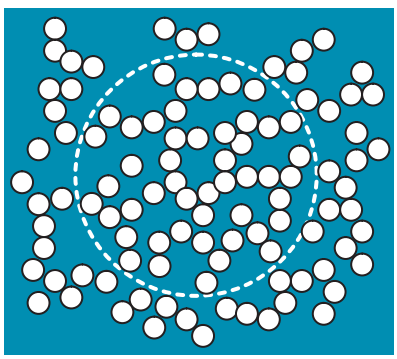

Figure 14. A schematic figure explaining the concepts of interaction network (transient gel) and bulk relaxation modulus. The dashed circle represents a membrane through which only liquid molecules can pass while particles (polymers or colloidal particles) (white balls) cannot. When we try to reduce or increase the local volume surrounded by the membrane with a speed faster than the relaxation rate of the bulk modulus, the membrane feels not only the osmotic stress but also the bulk mechanical stress. Note that bulk stress acts against osmotic stress; for example, if particles try to move via diffusion so as to increase their concentration inside the membrane, this motion inevitably stretches the network and thus bulk stress tries to prevent it. There are three physical origins of the bulk mechanical stress: (i) elasticity of the interaction network under the constraint of its connectivity; (ii) the topological constraint for particle motions, which originates from the connectivity of the interaction network; (iii) the topological constraint due to the excluded-volume effect of individual particles and hydrodynamic interactions. Origin (iii) plays few roles for polymer solutions, but plays important roles for colloidal suspensions.

chemical gels, polymer solutions and colloidal suspensions in a two-phase region and intuitively explain why the interaction network is responsible for bulk relaxation stress. For colloidal suspensions, there can be three physical origins of the bulk mechanical stress (see figure 14): (i) elasticity of the interaction network itself; (ii) the topological constraint for the motion of particles coming from the connectivity of the interaction network; (iii) the topological constraint for the motion of individual particles due to excluded-volume effects and strong hydrodynamic interactions. Note that origins (i) and (ii) also exist for polymer solutions and chemical gels, while origin (iii) does not play a crucial role for them in a typical concentration range.

5.3.3. Roles of bulk stress and the ϕ-dependent diffusion constant. Here we consider a naive, but quite important problem, namely, whether we should include the above effects of a transient gel in the ϕ-dependence of $\zeta(\phi)$ [73–76, 87, 88] or in the bulk stress [34, 108, 135]. Although they apparently cause similar effects, the physical mechanisms behind them are essentially different. The following simple criteria were proposed for this problem [135]:

(i) The friction with the 'local' rheological environment should be included in the ϕ-dependent mobility. The stress division parameter should also be determined by the general law of stress division, equation (46).
(ii) All the rheological effects arising from the interaction network should be included in the bulk and shear stresses. Note that the interaction network only exists in the phase-separation region.

Usually, the friction between the two components per volume, ζ, should simply depend upon ϕ, reflecting the probability of contacts between them per volume. In a two-fluid model of the polymer solutions, for example, even the effect of the chain connectivity of the polymer itself (entanglement effects) is included in the stress tensor via the constitutive equation of the polymer solution. All the non-local information should, thus, be expressed by the mechanical stress term in a two-fluid model.

Inclusion of the topological information, e.g., the connectivity of the interaction network, in the friction term suffers from the following two serious fundamental problems:

(i) It is not straightforward to include the dynamic effects in the diffusion constant. Note that the network tries to suppress diffusion only when the deformation rate exceeds the characteristic relaxation rate $1/\tau_{\mathrm{B}}$.
(ii) The friction term is introduced as a local term, but the connectivity produces 'non-local effects'.

Thus, the approach based on the bulk stress is physically more natural than that based on the ϕ-dependent diffusion constant for expressing the relaxational nature of a transient gel (origins (i)–(iii) listed in the caption of figure 14). Strictly speaking, the slow dynamics of a supercooled liquid associated with the liquid–glass transition can be described by a liquid-state theory but not by a solid-state theory. Note that a system is in a (supercooled) liquid state above the glass transition, although it has some solid-like character. The slow relaxation rate $1/\tau$ of a slow-component-rich phase should compete with the typical deformation rate associated with phase separation. The existence of a finite rheological timescale is quite an important feature of a liquid state. A solid state is, on the other hand, characterized by an infinite rheological timescale. It was shown by Jäckle [74–76] that rather gradual ϕ-dependence, e.g., the Vogel–Fulcher relation $D(\phi) \propto \exp[B/(\phi - \phi_{\mathrm{g}})]$, causes only weak effects and a much sharper ϕ-dependence was necessary to produce drastic effects including phase inversion. It is rather difficult to see how such a sharp ϕ-dependence for liquid–glass transition could arise since

usual theories of liquid–glass transition predict the above Vogel–Fulcher-type dependence. This fact may be viewed as an indication of the importance of the formation of a transient gel due to attractive interactions between like species in producing drastic viscoelastic effects such as phase inversion; a sharp ϕ-dependence of $D(\phi)$ might effectively mimic the formation of a transient gel.

In the solid model with ϕ-dependent mobility there are no effects of mechanical stresses and thus the true networklike structure, which satisfies the force-balance condition, is never formed, even though the pattern 'apparently' looks like a network structure. This is simply because there is no force-balance equation in solid models. More important, the initial stage of phase separation is not affected by any dynamic asymmetry for a solid model since the ϕ-dependence of the mobility is automatically dropped upon linearization of ϕ. If we include the elastic effects in a solid model, it leads to an entirely different pattern from a viscoelastic model (see section 9.4). Thus, we can conclude that *the fluid nature is essential for viscoelastic phase separation*. Practically, however, transient-gel effects may be introduced into a solid model by the sharp change in the ϕ-dependent mobility and such an approach may be useful especially in numerical simulations [73–76, 87].

5.3.4. Effective dynamic osmotic stress. Here we point out that the bulk stress cannot be included into the osmotic stress although the bulk stress originates from the intermolecular attractive interaction itself. This is due to a transient or dynamic nature of the bulk stress. In a permanent gel, for example, the bulk stress term can be naturally included in the osmotic stress, π, since the elastic energy term can be included in the free energy of a system. Formally, however, we can include the bulk stress in the effective dynamic osmotic stress as

$$\pi^{\rm eff}(t) = \phi(\partial f/\partial\phi) - f - \int_{-\infty}^{t} {\rm d}t'\, G_{\rm B}(t-t')(\boldsymbol{\nabla}\cdot\boldsymbol{v}_{\rm r}(t')). \tag{47}$$

Obtaining the theoretical expression for the dynamic osmotic stress in a non-equilibrium state is a challenging theoretical problem. It may be interesting to compare the above with the approach described in section 4.1.2.

6. Generality of a viscoelastic model

Next we briefly discuss the generality of the above viscoelastic model described by equations (40), (41) and (42) [34]. This model including the bulk volume relaxation mode is a quite general model, as shown below. We describe below how the viscoelastic model reduces to various models under certain assumptions.

6.1. The elastic solid model

If we assume that $G_{\rm S}(t) = \mu(\phi)$ (μ: shear modulus) ($\tau_{\rm S} = \infty$) and $G_{\rm B}(t) = K_{\rm b}(\phi)$ ($K_{\rm b}$: bulk modulus) ($\tau_{\rm B} = \infty$) and $\boldsymbol{v} = 0$, this model reduces to the elastic solid model [144]. Since the time integration of the velocity becomes the deformation u, the stress is given by

$$\sigma_{ij}^{(k)} = \mu^{(k)}(\phi)\left[\frac{\partial u_j^{(k)}}{\partial x_i} + \frac{\partial u_i^{(k)}}{\partial x_j} - \frac{2}{d}(\boldsymbol{\nabla}\cdot\boldsymbol{u}^{(k)})\delta_{ij}\right] + K_b^{(k)}(\phi)(\boldsymbol{\nabla}\cdot\boldsymbol{u}^{(k)})\delta_{ij}. \tag{48}$$

Thus, the basic kinetic equation is obtained as

$$\frac{\partial\phi}{\partial t} = \boldsymbol{\nabla}\cdot\frac{\phi(1-\phi)^2}{\zeta(\phi)}\left[\boldsymbol{\nabla}\cdot\boldsymbol{\Pi} - \boldsymbol{\nabla}\cdot\boldsymbol{\sigma}^{(1)} + \frac{\phi}{1-\phi}\boldsymbol{\nabla}\cdot\boldsymbol{\sigma}^{(2)}\right]. \tag{49}$$

In this case, the softer phase forms a networklike phase because the deformation of the softer phase costs less energy than that of the harder phase [144]. It should be stressed that the force-balance condition plays no role in determining the morphology. This fact causes the striking difference in morphology between an elastic solid model and an elastic gel or asymmetric viscoelastic model [32]: in the former the softer phase forms the networklike structure, while in the latter the harder phase does this (see section 9.4).

6.2. The solid model

If we further assume dynamic symmetry (no dependence of μ and K_b on ϕ), it reduces to the solid model (model B [4]). This is because we have the symmetric stress division $(1-\phi)\boldsymbol{F}_1 = \phi\boldsymbol{F}_2$. Here it should be noted that the condition $\mu = K_b = 0$ is unnecessary for deriving this model and only the symmetry in elastic properties of the two components is required. In this case, the basic equation becomes the simplest diffusion equation:

$$\frac{\partial\phi}{\partial t} = \boldsymbol{\nabla}\cdot\frac{\phi(1-\phi)^2}{\zeta(\phi)}[\boldsymbol{\nabla}\cdot\boldsymbol{\Pi}]. \tag{50}$$

6.3. The symmetric viscoelastic model

If we assume only dynamic symmetry between the two components of a mixture, the viscoelastic model reduces to a 'symmetric viscoelastic model'. In this case, we have a trivial stress division: $\boldsymbol{F}_1 = \phi\boldsymbol{\nabla}\cdot\boldsymbol{\sigma}$ and $\boldsymbol{F}_2 = (1-\phi)\boldsymbol{\nabla}\cdot\boldsymbol{\sigma}$. That is, $\alpha_1 = \phi$ and $\alpha_2 = 1-\phi$. The rheological functions $G_j^{(k)}$ can be estimated as $G_j^{(1)}(t) = \phi G_j(t)$ and $G_j^{(2)}(t) = (1-\phi)G_j(t)$. In this particular case, $\boldsymbol{v}_r = \boldsymbol{v}$; and, accordingly, there should be no contribution of the bulk relaxation modulus under the incompressibility condition ($\boldsymbol{\nabla}\cdot\boldsymbol{v} = 0$). The basic kinetic equations are given by

$$\frac{\partial\phi}{\partial t} = -\boldsymbol{\nabla}\cdot(\phi\boldsymbol{v}) + \boldsymbol{\nabla}\cdot\frac{\phi(1-\phi)^2}{\zeta}\boldsymbol{\nabla}\cdot\boldsymbol{\Pi} \tag{51}$$

$$\rho\frac{\partial\boldsymbol{v}}{\partial t} \cong -\boldsymbol{\nabla}\cdot\boldsymbol{\Pi} + \boldsymbol{\nabla}p + \boldsymbol{\nabla}\cdot\boldsymbol{\sigma}. \tag{52}$$

Since $\boldsymbol{v}_r = \boldsymbol{v}$, the gross variables describing the dynamics are only ϕ and $\boldsymbol{v}$. Here it should be stressed that the rheological function $G(t)$ does not depend upon the location $\boldsymbol{r}$ because of the dynamic symmetry. Using the relation $\boldsymbol{\nabla}\cdot\boldsymbol{v} = 0$, thus,

$$\boldsymbol{F} = \boldsymbol{\nabla}\cdot\boldsymbol{\sigma} = \int_{-\infty}^{t} \mathrm{d}t'\, G(t-t')\,\nabla^2\boldsymbol{v}(t'). \tag{53}$$

For example, this model can describe the dynamics of dynamically symmetric polymer mixtures. The unusual behaviour is expected in the initial stage of phase separation where the deformation rate is large ($t < \tau_t$).

6.4. The fluid model

If we assume that the deformation changes much more slowly than the internal rheological time of the material for the above model, we further have the relation $\boldsymbol{\nabla}\cdot\boldsymbol{\sigma} = \eta\,\nabla^2\boldsymbol{v}$. Thus, the model reduces to the fluid model (model H [4]):

$$\frac{\partial\phi}{\partial t} = -\boldsymbol{\nabla}\cdot(\phi\boldsymbol{v}) + \boldsymbol{\nabla}\cdot\frac{\phi(1-\phi)^2}{\zeta}\boldsymbol{\nabla}\cdot\boldsymbol{\Pi} \tag{54}$$

$$\rho\frac{\partial\boldsymbol{v}}{\partial t} \cong -\boldsymbol{\nabla}\cdot\boldsymbol{\Pi} + \boldsymbol{\nabla}p + \eta\,\boldsymbol{\nabla}^2\boldsymbol{v}. \tag{55}$$

6.5. The elastic gel model

If we just assume $G_S = \mu(\phi)$ and $G_B = K_b(\phi)$, it reduces to the elastic gel model [57, 59] that describes phase separation in elastic gel. The basic equations are essentially the same as those of viscoelastic phase separation in polymer solution (equations (40), (41) and (42)), except that the stress tensor is given by

$$\sigma_{ij}^{(1)} = \mu(\phi)\left[\frac{\partial u_1^j}{\partial x_i} + \frac{\partial u_1^i}{\partial x_j} - \frac{2}{d}(\boldsymbol{\nabla}\cdot\boldsymbol{u}_1)\delta_{ij}\right] + K_b(\phi)(\boldsymbol{\nabla}\cdot\boldsymbol{u}_1)\delta_{ij}$$

$$\sigma_{ij}^{(2)} = \eta_2\left[\frac{\partial v_2^j}{\partial x_i} + \frac{\partial v_2^i}{\partial x_j} - \frac{2}{d}(\boldsymbol{\nabla}\cdot\boldsymbol{v}_2)\delta_{ij}\right].$$

In this case, when the elastic energy overcomes the mixing free energy, the coarsening of domains may stop due to elastic pinning effects.

6.6. Generality and intrinsic non-universality

6.6.1. Generality of the viscoelastic model. Since any descriptions of phase separation in all isotropic condensed matter can be classified into solid, elastic solid, elastic gel, symmetric and asymmetric viscoelastic and fluid models, the above viscoelastic model including both shear and bulk relaxation stresses should be a universal model, which can describe phase separation and critical phenomena in isotropic matter without any exception [34].

Usually material is classified into the following three types: fluid, viscoelastic matter and solid. The criterion is given by the relation between the internal rheological time τ_t and the observation time τ_o, as shown in figure 15. It was proposed [34] that corresponding to this mechanical classification of material, descriptions of phase separation can be classified into the following three models: fluid, viscoelastic and solid models. In this case, the criteria are based on whether there are the velocity fields and dynamic asymmetry. Note that the

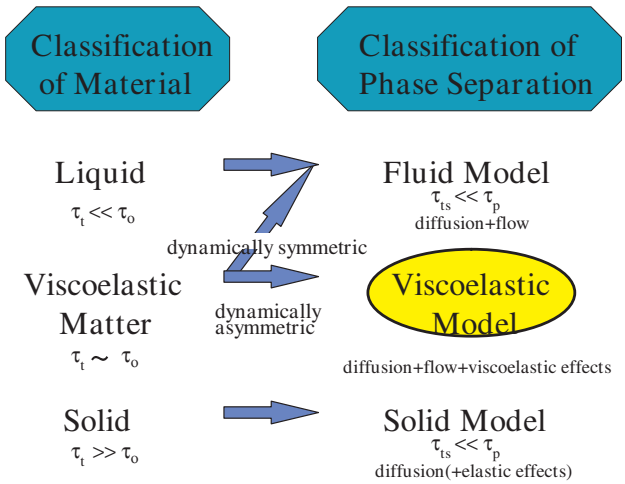

Figure 15. Classification of material on the basis of rheological properties and the corresponding classification of descriptions of phase separation. The criterion for the former classification is given by the relation between the internal rheological time τ_t and the observation time τ_o. For the latter classification, on the other hand, it is given by the dynamic asymmetry in addition to the relation between τ_t and τ_o.

viscoelastic model includes solid and fluid models as special cases, as shown above, similarly to viscoelastic matter including solid and fluid as special cases.

6.6.2. Non-universality. Despite the generality, the viscoelastic model is not universal in the usual sense of critical phenomena since it requires some microscopic theories describing the rheological properties of the matter. In the extreme limit of strong dynamic asymmetry, the elementary slow dynamics (internal mode) of the material affects critical fluctuations even near the critical point, in conflict with the concept of dynamic universality [4]. As an example, we consider the case of polymer solutions [32]. For polymer solutions, we can control the dynamic asymmetry by changing the degree of polymerization of the polymer, N. In the limit of $N \to \infty$, $\tau_t \to \infty$. In this limit, further, $T_t \to T_c$ (see figure 6). Note that $T_c = T_\theta$ (T_θ: θ-temperature) for $N = \infty$. Thus, there arises the interesting situation that τ_t is always shorter than or comparable to the characteristic lifetime of concentration fluctuations τ_ξ. Note that static features such as the correlation length ξ and the scattering intensity are not affected by viscoelastic effects and only the dynamics is affected. For such a case, the dynamic universality breaks down since there are two relevant timescales (τ_ξ and τ_t) and two relevant length scales associated with them (ξ and ξ_{ve}). The viscoelastic length is given by $\xi_{ve} \sim (D_\xi \tau_t)^{1/2}$, where τ_t is the characteristic time of rheological relaxation and D_ξ is the diffusion constant. For the length scale longer than ξ_{ve}, concentration fluctuations decay by diffusion, while for the length scale shorter than ξ_{ve}, viscoelastic effects dominate [93,100,101]. This is a simple time-to-space mapping of the dynamic crossover whereby on a timescale longer than τ_t, diffusion dominates concentration fluctuations while on a timescale shorter than τ_t, viscoelastic effects dominate. The critical regime is, thus, described by the condition $\xi \gg \xi_{ve}$. This condition can also be written as $\tau_\xi \gg \tau_t$. Thus, we need to consider whether we can easily approach the critical regime that is defined by the above criterion, in a viscoelastic system. In many cases, thus, there is a possibility that we cannot experimentally approach a critical regime where the order parameter dynamics is the only slow mode in the system [30–32].

The same consideration can also be applied to phase separation. Theoretically, the true late-stage coarsening should be described by a fluid model even for a dynamically asymmetric mixture. Experimentally, accessing this asymptotic coarsening regime in phase separation may be easier than accessing the true critical regime in dynamic critical phenomena, simply because there is no experimental limitation on the phase-separation time.

The existence of the viscoelastic relaxation mode predicted by Brochard and de Gennes was observed by Brown and co-workers [145, 146] for polymer solutions. However, there remains some controversy as regards this problem [147] and thus further studies are required to clarify the viscoelastic effects on the critical phenomena. The viscoelastic suppression of the critical anomaly was recently suggested for polymer solutions on the basis of viscosity measurements [31,32,148,149]. Finally, it may be worth mentioning an interesting possibility that the viscoelastic effects on critical phenomena may be directly detected by means of depolarized light scattering [150].

7. Viscoelastic phase separation: theoretical predictions and interpretations

7.1. The early stage of viscoelastic phase separation

7.1.1. The solid model with ϕ-dependent mobility. In this case (see equation (1)), it is obvious that the linearized version of the equation reduces to Cahn's equation given by equation (5). Thus, we do not expect any new effects associated with the ϕ-dependent mobility for this type of model. This is quite different from the case for a two-fluid model. As shown in section 4.1,

however, the additional slow dynamics was introduced into a solid model by Binder *et al* [65] and this particular model predicts a very similar behaviour to the following two-fluid model, as mentioned before.

7.1.2. A two-fluid model: spinodal decomposition. The early stage of viscoelastic phase separation was studied by Doi and Onuki [100], Onuki [109], Onuki and Taniguchi [151] and Kumaran and Frederickson [152] on the basis of the linearized two-fluid model. Here we briefly summarize the predictions [100, 109, 151] for the case where only a pure shear modulus exists ($G_B = 0$).

Using the relation $\boldsymbol{\nabla} \cdot \boldsymbol{v}_r = -\alpha\ \partial\phi/\partial t$, we obtain the linearized equation for $Z_q = [\boldsymbol{\nabla} \cdot \boldsymbol{\nabla} \cdot \boldsymbol{\sigma}]_q$ from equation (33):

$$\frac{\partial Z_q}{\partial t} \simeq -\frac{Z_q}{\tau} + \frac{4G_S}{3}\alpha q^2 \frac{\partial \phi_q}{\partial t}$$

where $\alpha = \alpha_1 - \alpha_2$ is the dynamic asymmetry parameter. Here ϕ_q is the Fourier component of the deviation from the initial composition ϕ_0, and it obeys, to linear order [100, 151],

$$\frac{\partial \phi_q(t)}{\partial t} \simeq -\Gamma_q \phi_q(t) - \frac{4}{3}\alpha^2 L G_S q^2 \int_0^t \mathrm{d}t'\ \exp\left(-\frac{t-t'}{\tau}\right)\frac{\partial \phi_q(t')}{\partial t'}. \tag{56}$$

Here $\Gamma_q = Lq^2(-r + Cq^2)$, where $L = \phi^2(1-\phi)^2/\zeta(\phi)$, is the decay rate in the absence of the viscoelastic coupling. The correlation length is given by $\xi = [C/|r|]^{1/2}$.

For a case where the timescale of ϕ_q is longer than τ, we can set

$$\frac{\partial \phi_q(t')}{\partial t'} = \frac{\partial \phi_q(t)}{\partial t}$$

in equation (56) and, thus, the growth rate of ϕ_q is given by

$$A(q) = L|r|q^2(1 - \xi^2 q^2)/(1 + \xi_{ve}^2 q^2) \tag{57}$$

where $\xi_{ve} = (\frac{4}{3}\alpha^2 \eta L)^{1/2}$ is the so-called viscoelastic length [93, 100, 101]. Note that $G_S \sim \eta/\tau$. This ξ_{ve} gives us the length scale above which the dynamics is dominated by diffusion and below which it is dominated by viscoelastic effects. Without viscoelastic coupling, the relation $A(q) = L|r|q^2(1 - \xi^2 q^2)$ should hold, as Cahn's linear theory [1] predicts (see section 2.1.1).

Figure 16 indicates [135] that the above relation (equation (57)) explains well the unusual q-dependence of $A(q)$ experimentally observed in colloid phase separation [121]. In this case, ξ_{ve} is determined as $\xi_{ve} \sim 10\xi \sim 2.4\ \mu$m by the fitting. Although further careful studies are required, this suggests the relevance of a two-fluid model. Similar analysis may also be applied to the early stage of phase separation of polymer systems [153–155].

In the opposite limit of $\tau \gg 1/\Gamma_q$, the system behaves as a gel and we have

$$A_{gel}(q) = \Gamma_q + \frac{\xi_{ve}^2 q^2}{\tau} = Lq^2\left(-r + \frac{4}{3}\alpha^2 G_S + Cq^2\right). \tag{58}$$

If $|r| > \frac{4}{3}\alpha G_S$, the system is unstable even on a timescale shorter than τ. This situation is analogous to that of a gel in the spinodal region [59] where $K_{os} + \frac{4}{3}G_S < 0$. Here $K_{os} = \phi(\partial\pi/\partial\phi)_T$ is the osmotic bulk modulus.

Here it should be noted that even a pure shear modulus affects the early stage of phase separation, as described above. This is because the plane composition wave (1D sinusoidal wave) characteristic of the linear stage accompanies the longitudinal deformation, which is characterized by the longitudinal modulus $L = G_B + \frac{4}{3}G_S$. Even for $G_B = 0$, L is finite. For a usual simple network system, $G_B = \frac{2}{3}G_S$ and $L = 2G_S$. However, it should be stressed that the pure shear modulus never produces volume-shrinking behaviour or phase-inversion

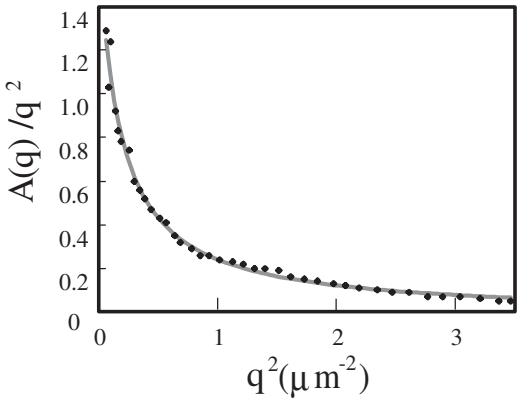

Figure 16. Fitting of equation (16) to the experimentally observed growth rate of concentration fluctuations, $A(q)$. The solid curve represents a theoretical curve. The data were taken from reference [121].

behaviour [34, 108], since it does not couple to the diffusion mode of the slow component 1 with a spherical symmetry, or the deformation of type $\boldsymbol{\nabla} \cdot \boldsymbol{v}_1$. We need the bulk modulus (non-zero G_{B}) to explain the volume-shrinking behaviour, as shown below.

7.1.3. A two-fluid model: nucleation and growth. A nucleation and growth process under the influence of viscoelastic effects was studied by Onuki [109, 156]. He considered the growth of a spherical domain of nearly pure solvent in a metastable semidilute polymer region. In such a case, the surrounding semidilute region is deformed in the radial direction, which gives rise to a large viscoelastic stress. Thus, the Gibbs–Thomson relation should be modified as

$$\pi - \sigma_n + 2\Gamma/R = \pi_{\mathrm{cx}}. \tag{59}$$

Here π is the osmotic pressure, $\sigma_n = \boldsymbol{n} \cdot \boldsymbol{\sigma} \cdot \boldsymbol{n}$ is the normal component of the network stress in the normal direction $\boldsymbol{n}$, R is the droplet radius and π_{cx} is the osmotic pressure on the coexistence curve. For the case where the growth takes much longer than τ, a modified Lifshitz–Slyozov equation is obtained as

$$\dot{R} = \frac{2\sigma}{\zeta R}\left(\frac{1}{R_{\mathrm{c}}} - \frac{1}{R}\right)\Big/\left(1 + 3\frac{\xi_{\mathrm{ve}}^2}{R^2}\right) \tag{60}$$

where R_{c} is the critical radius and σ is the interface tension. Note that $\xi_{\mathrm{ve}} = (4\eta/3\zeta)^{1/2}$. For $R \ll \xi_{\mathrm{ve}}$, thus, the viscoelastic effects decelerate the droplet growth, while for $R \gg \xi_{\mathrm{ve}}$ the growth should be described by the usual Lifshitz–Slyozov equation.

Although there have been several experiments on nucleation and growth in polymer solutions [157–160], few experiments have focused on viscoelastic effects. Further studies are highly desirable, to help us to understand how the viscoelastic effects affect the nucleation–growth kinetics.

7.2. Suppression of diffusion due to the bulk relaxation modulus

According to the continuity equation, equation (1), we have the following relation:

$$\frac{\partial \phi(\boldsymbol{r}, t)}{\partial t} = -\boldsymbol{\nabla}\phi(\boldsymbol{r}, t) \cdot \boldsymbol{v}_1(\boldsymbol{r}, t) - \phi(\boldsymbol{r}, t)\, \boldsymbol{\nabla} \cdot \boldsymbol{v}_1(\boldsymbol{r}, t). \tag{61}$$

Here we assume that component 1 is a slow component such as polymer and component 2 is a fast component such as a solvent. ϕ is the composition of component 1. In the above equation, the first term on the right-hand side simply describes the translational transport of polymers to a point $\boldsymbol{r}$ by the local velocity field $\boldsymbol{v}_1$, while the second one describes the diffusion of component 1 towards or away from a point $\boldsymbol{r}$. Thus, the first term is associated only with the change in the spatial pattern of the concentration distribution, while the second term is responsible for the change in the concentration distribution itself. Only the second term is relevant to the diffusion process, which leads to the change in the concentration distribution itself.

Neglecting the first term in equation (61), thus, we have the relation

$$\frac{\partial \phi}{\partial t} \Big/ \phi \cong -\boldsymbol{\nabla} \cdot \boldsymbol{v}_1. \tag{62}$$

The left-hand side of the above equation is inversely proportional to the characteristic time of the concentration change, τ_ϕ. On the other hand, the bulk relaxation modulus $G_{\mathrm{B}}(t)$ that is directly coupled with $\boldsymbol{\nabla} \cdot \boldsymbol{v}_1$ has a characteristic decay time of τ_{B}, which is related to the characteristic time of the transient gel. Note that a pure shear mode is never coupled with $\boldsymbol{\nabla} \cdot \boldsymbol{v}_1$. If $\tau_{\mathrm{B}} \gg \tau_\phi$, the rapid growth of concentration fluctuations characteristic of spinodal decomposition is severely suppressed and may even be prohibited. If $\tau_{\mathrm{B}} \ll \tau_\phi$, on the other hand, there are few elastic effects and the concentration fluctuations can grow as in usual spinodal decomposition. The crossover from an initial fluid state to a transient-gel state takes place in a rather early stage of spinodal decomposition after the temperature quench. After the formation of a transient gel, the 'mechanical instability' that is a universal feature of the 'soft' network of attractive interactions leads to the apparently nucleation–growth-like behaviour. In the following, we discuss the concept of 'order parameter switching' resulting from the crossover between the characteristic phase-separation time and the internal rheological time.

7.3. Intermediate and late stages: order parameter switching

7.3.1. Order parameter switching between the composition and the deformation tensor. Here we consider the dynamic process of viscoelastic phase separation on the basis of the viscoelastic relaxation phenomena described by equation (33). The quantitative feature of the dynamics can be understood on the basis of a concept of 'order parameter switching' [33, 34]. Phase separation is usually driven by a thermodynamic force and the resulting ordering process can be described by the temporal evolution of the relevant order parameter associated with the thermodynamic driving force. The primary order parameter describing phase separation of a binary mixture is the composition difference between the two phases. Other than in exceptional cases where phase separation and other ordering processes such as superfluidization, gelation, liquid crystallization and crystallization proceed simultaneously [1] (in other words, there are more than two kinds of thermodynamic force (order parameters)), a phase-separation process is usually characterized by a single order parameter. In the viscoelastic model, on the other hand, the phase-separation mode can be switched between the 'fluid mode' and the 'elastic gel mode'. This switching is caused by the change in the coupling between stress and velocity fields, which is described by equation (33): equation (33) tells us that the two ultimate cases, namely, (i) the fluid model (κ_{ij}^p, $\boldsymbol{\nabla} \cdot \boldsymbol{v}_{\mathrm{r}} \sim$ constant) and (ii) the elastic gel model ($G_{\mathrm{S}}(t)$, $G_{\mathrm{B}}(t) \sim$ constant), correspond to $\tau_{\mathrm{d}} \gg \tau_{\mathrm{ts}}$ and $\tau_{\mathrm{d}} \ll \tau_{\mathrm{ts}}$, respectively. Here τ_{d} is the characteristic time of deformation and τ_{ts} is the characteristic rheological time of the slower phase.

For $\tau_{\mathrm{d}} \gg \tau_{\mathrm{ts}}$ the primary order parameter is the composition in usual classical fluids, while for $\tau_{\mathrm{d}} \leqslant \tau_{\mathrm{ts}}$ it is the deformation tensor ($d_{ij} = \partial u_j/\partial x_i + \partial u_i/\partial x_j$) as in elastic gels. In the elastic regime, the force terms can be included in the Hamiltonian as for the case of gel. Then the

free-energy functional is formally written just in terms of the deformation tensor d_{ij} as $f(d_{ij})$. Thus, we can say that the order parameter switching is a result of the competition between the two timescales characterizing domain deformation, τ_d, and the rheological properties of domains, τ_{ts}. This is a kind of *viscoelastic relaxation* in pattern evolution.

7.3.2. How does the order parameter switching occur? We next consider how τ_{ts} and τ_d change with time during phase separation [33, 34]. In the initial stage, the velocity fields grow as $v \sim (k_B TC/3\eta\xi)\,\Delta\phi^2$, where $\Delta\phi$ is the composition difference between the two phases and ξ is the correlation length, or the interface thickness. Since $\Delta\phi$ approaches $2\phi_e$ (ϕ_e: the equilibrium composition) with time, this expression for v reduces to the well-known relation $v \sim \sigma/\eta$ in the late stage (note that $\sigma \sim k_B TC(2\phi_e)^2/3\xi$). Thus, the characteristic deformation time τ_d changes with time as $\tau_d \sim R(t)/v(t) \sim R(t)/\Delta\phi(t)^2$. In the initial stage, the domain size does not grow so much with time while $\Delta\phi$ rapidly increases with time; and, accordingly, τ_d decreases rapidly. On the other hand, τ_{ts} increases steeply with increase in $\Delta\phi$, reflecting the increase in the polymer concentration in a polymer-rich domain. Thus, τ_{ts} becomes comparable to τ_d in the intermediate stage of phase separation. Once $\tau_d < \tau_{ts}$, the slower phase cannot follow the deformation speed and behaves as an elastic body: the elastic energy dominates the coarsening process in the intermediate stage. Next we consider the late stage. Since $\Delta\phi$ approaches $2\phi_e$ and becomes almost constant in the late stage, τ_d ($\sim R\eta/\sigma$) increases with increase in R while τ_{ts} becomes almost constant. Thus, τ_d becomes longer than τ_{ts} again. In short, $\tau_d \gg \tau_{ts}$ in the initial stage, $\tau_d \leqslant \tau_{ts}$ in the intermediate stage and $\tau_d \gg \tau_{ts}$ in the late stage again. Accordingly, the order parameter switches from the composition to the deformation tensor and then switches back to the composition again. The situation is schematically shown in figure 17. This is a rare case of 'order parameter switching' during an ordering process driven by a single thermodynamic driving force.

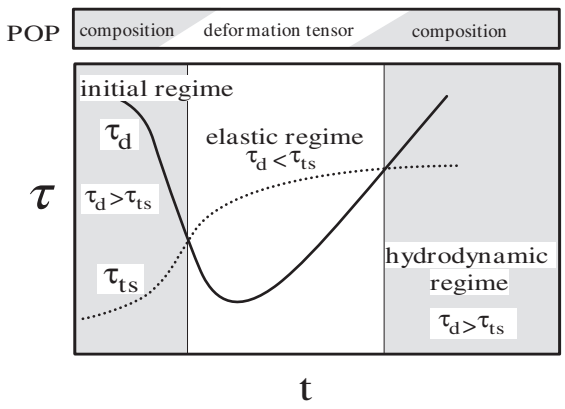

Figure 17. A schematic figure explaining the concept of the order parameter switching. The upper figure indicates the primary order parameter (POP). The lower figure indicates the temporal change in the characteristic timescales of phase separation and internal rheological time.

7.3.3. Kinetics of transient-gel formation. Here we briefly consider how viscoelastic functions, $G_S(t)$ and $G_B(t)$, emerge, reflecting the formation of a transient gel. In the above discussion, τ_{ts} is assumed to be a function of $\Delta\phi$ only. However, this picture is not necessarily correct. In polymer solutions and colloidal suspensions, for example, a transient gel should be formed very quickly after the quench. This is because the diffusion of polymers or colloidal

particles over a large length scale is not required to form the interaction network. The diffusion length scale l is of the order of the polymer or particle size, a, near the critical composition (ϕ_c); and, thus, the time required to form a network is $\sim a^2/D_a$, where D_a is the diffusion constant of a polymer or particle. In such a case, τ_{ts} very rapidly increases to the order of τ_d within a time of $\sim a^2/D_a$ after the quench. In such a case, the first order parameter switching from composition to deformation tensor occurs within a very short period ($\sim a^2/D_a$) after the quench: the system enters an elastic regime just after the quench. The early stage of phase separation may be viewed as the process of the competition between spinodal decomposition and transient-gel formation. This is related to the basic problem of what the difference is between 'aggregation' and 'phase separation', both of which are induced by attractive interactions. This initial process of viscoelastic phase separation cannot be described by the coarse-grained model such as the viscoelastic model in the exact sense. The term 'aggregation' seems to be used when a coarse-grained phase-separation model cannot be applied. A mesoscopic or microscopic model is required for the precise description of such an aggregation process including the temporal change in the viscoelastic functions, $G_S(t)$ and $G_B(t)$.

The diffusion length scale l increases with decrease in polymer or colloid concentration ϕ. If a percolated network cannot be formed within a sufficiently short time, a percolated network with an infinite size is never realized due to phase separation and, thus, a networklike phase-separated pattern is not formed; instead, a droplet pattern is formed [29,30]. This criterion may give the threshold composition between droplet and network phase separation (see figure 6).

7.3.4. Elasticity of the interaction network. The physical origin of the existence of $G_B(t)$ and the fact that bulk stress competes with osmotic stress need further considerations. Suppose that we have an infinite percolated network. Now the interaction network far from equilibrium tries to shrink its effective volume in order to lower the free energy. However, any non-uniform deformation of the network costs elastic energy due to its connectivity. This is the origin of the bulk mechanical stress. Note that although the interaction network is not stable in the global sense, it is locally stabilized by the attractive interaction between the components. What is behind this intuitive explanation is the self-induced constraint due to the connectivity of the elastic network. *This constraint is mathematically equivalent to the following boundary condition for a finite system: the network velocity* $\boldsymbol{v}_n$ *at the boundary is zero.* This can be experimentally realized by bonding the slow components to the boundary, e.g., chemical gel attached to a gel-bond film. This condition is automatically satisfied whenever the network is interconnected and not isolated. Note that osmotic stress, or diffusion, tries to create and enhance inhomogeneity during phase separation. Thus, this bulk stress effect against diffusion should exist universally whenever there is a large difference in relaxation rate of the interaction network between the two components.

This scenario can be explained by the following force density acting on the elastic network:

$$\boldsymbol{F}_n = -\boldsymbol{\nabla}\cdot\boldsymbol{\Pi} + \boldsymbol{\nabla}\cdot\boldsymbol{\sigma}. \tag{63}$$

A gel upon shrinking or swelling from a relaxed state or a transient gel always tries to avoid deformation. In other words, a transient gel is in a state of marginal balance where the osmotic force tries to shrink the network by diffusion to lower the free energy, but the bulk stress force tries to cancel it. Accordingly, the total net force acting on the network is strongly suppressed. This picture intuitively explains the role of bulk stress. The above argument also justifies the way of introducing the bulk stress as in equations (33); that is, we should take a natural length of a spring as the length of spring just after the formation of a transient gel. It is the connectivity that prevents a network from collapsing.

There are two types of pattern evolution for a (transient) gel with a free boundary,

depending upon its size: (a) shrinking homogeneously and (b) shrinking inhomogeneously under the strong influence of mechanical stress. Process (a) may occur only when the system size R is so small that the characteristic diffusion time $\tau_D = R^2/D$ (D: diffusion constant) is shorter than the characteristic bulk mechanical relaxation time τ_B. In other words, the viscoelastic length ξ_{ve} is larger than R. This condition ensures that a gel is free from the constraint of interconnectivity. In this case, the mechanical instability (or nucleation) may be avoided. This means that there is a critical size of a gel below which the gel can shrink rather homogeneously without mechanical instability. However, the formation of a skin layer, which is a shrunken phase at the boundary, may encourage bulk mechanical instability. It is interesting to check these points experimentally for chemically crosslinked permanent gels.

In all other cases, process (b), or mechanical instability, inevitably occurs. The competition between osmotic stress and bulk stress plays a key role in pattern evolution during phase separation. Elasticity of the network does not favour any deformation. Thus, the only way to achieve it during phase separation is to localize the deformation at the interface (or boundary) of domains. This leads to the suppression of the normal diffusion. The diffusion modes whose wavelengths are shorter than ξ_{ve} are always strongly suppressed. Thus, the diffusion process must accompany the volume shrinking of a more elastic phase to avoid the inhomogeneous deformation of a network. The localization of bulk stress at the periphery of a more elastic phase and the volume shrinking are confirmed in our simulation [161].

The local stretching caused by the shrinking of a transient gel leads to the stress concentration on the stretched part of a domain and leads to its break-up, which further enhances the inhomogeneous stress distribution. Thus, the process of phase separation accompanying the shrinking of an interaction network can be viewed as *mechanical instability of a network formed by non-linear springs*.

7.3.5. Volume-shrinking behaviour: the absence of self-similar pattern growth in viscoelastic phase separation. We briefly discuss the physical origin of the formation of sponge structure, or relative volume shrinking of a more viscoelastic phase. This is related to the fact that in a two-fluid model $\nabla \cdot \boldsymbol{v}_k$ need not be zero even under the incompressibility condition $\nabla \cdot \boldsymbol{v} = 0$ for the average velocity. There are three important factors in this problem:

(i) whether the component k is compressible in a mixture, or not;
(ii) whether $\nabla \cdot \boldsymbol{v}_1$ is large enough or not; and
(iii) whether the change in $\nabla \cdot \boldsymbol{v}_k$ is properly coupled with the stress, or not.

Condition (i) is usually satisfied in a mixture, one of whose components is 'fluid', since the spatial configuration of a component can be changed by its own velocity fields. Condition (ii) is also satisfied only for a system containing a fluid as a component. Finally, condition (iii) is satisfied when there exist both attractive interactions between the components and strong dynamic asymmetry. In a simple fluid mixture, for example, $\nabla \cdot \boldsymbol{v}_k$ is not coupled with the elastic stress even if there is a difference in viscosity between the two components.

It can be concluded that the bulk mechanical relaxation modulus $G_B(t)$ plays an essential role in the volume-shrinking behaviour, while the shear modulus G_S does not play a primary role. To prevent the usual spinodal decomposition from taking place, on the other hand, the longitudinal modulus L should be sufficiently large. The growth of the concentration fluctuations has to be suppressed mainly by $\nabla \cdot \boldsymbol{v}_k$. This is realized by the formation of a transient gel (or the interaction network). The long-range nature of the elastic interaction in a more viscoelastic phase is directly related to how efficiently the fluctuations are suppressed and the volume of the relevant phase can be changed and, thus, to the ability to form spongelike structure.

Because of the order parameter switching, there is no self-similarity in the pattern evolution of viscoelastic phase separation. In the elastic regime, further, the apparent volume ratio between the two phases changes with time [30, 33]; and, thus, there is no proportionality between interdomain distance and domain size. This behaviour even leads to phase inversion when the more viscoelastic phase is slightly a minority phase in equilibrium—that is, in the composition range between the DSL and the SSL (see figure 6). In the initial stage, a less viscoelastic phase forms droplets, while in the final stage, a more viscoelastic phase does this.

7.3.6. Roles of the shear relaxation modulus in the formation of a networklike structure. Next we focus our attention on the roles of the shear relaxation modulus. An important fact is that the bulk relaxation modulus is closely related to the diffusion, while the shear relaxation modulus is not: the bulk stress gradient, $\boldsymbol{\nabla} \cdot \boldsymbol{\sigma}_{\mathrm{B}}$, is usually (at least in the initial stage) in the same orientation with respect to the osmotic stress gradient, $\boldsymbol{\nabla} \cdot \boldsymbol{\Pi}$, since both are related to the diagonal part of the deformation velocity, $\boldsymbol{\nabla} \cdot \boldsymbol{v}_{\mathrm{r}}$, as described before. On the other hand, the shear stress gradient, $\boldsymbol{\nabla} \cdot \boldsymbol{\sigma}_{\mathrm{S}}$, is usually not in the same orientation with respect to $\boldsymbol{\nabla} \cdot \boldsymbol{\Pi}$, since it is related to the off-diagonal part of the deformation velocity. Thus, the shear relaxation modulus plays a dominant role in the formation of a networklike structure in the intermediate stage of viscoelastic phase separation. The overlapping of the stress fields having spherical symmetry around a spherical solvent hole induces deformation of shear type. This initial spherical symmetry of the stress field is characteristic of the bulk stress fields coupled with $\boldsymbol{\nabla} \cdot \boldsymbol{v}_{\mathrm{r}}$. The shear deformation causes the shear stress fields through the shear relaxation modulus. Thus, the thin part of a more viscoelastic phase supports the shear stress and is elongated further. In other words, the existence of a shear relaxation modulus is responsible for the formation of a 'networklike' pattern composed of highly elongated thin structures [161]. The network structure is basically determined by the force-balance condition. Without a shear relaxation modulus, the 'networklike' pattern with threadlike structures can never be formed (see the simulation results in section 8).

7.3.7. Pattern selection: elastic energy versus interface energy. Since the deformation tensor intrinsically has a geometrical nature, the pattern in the elastic regime is essentially different to that of usual phase separation in fluid mixtures. The domain shape during viscoelastic phase separation is determined by which of the elastic and interface energy is more dominant. Roughly, the elastic energy is estimated as $\mu e^2 R^d$ (μ: elastic modulus; e: strain; and d: spatial dimensions) for a domain of size R, since it is the bulk energy. On the other hand, the interface energy is estimated as σR^{d-1}. For macroscopic domains, thus, the elastic energy is always much more important than the interface energy in the intermediate stage where $\tau_{\mathrm{d}} \leqslant \tau_{\mathrm{ts}}$. Accordingly, the domain shape is determined by the elastic force-balance condition ($\boldsymbol{\nabla} \cdot \boldsymbol{\sigma}^{\mathrm{n}} \sim 0$), which leads to networklike or spongelike morphology. This explains the frequent appearance of three-arm structures in 2D and four-arm structures in 3D. In the late stage of phase separation where $\tau_{\mathrm{d}} \gg \tau_{\mathrm{ts}}$, on the other hand, the interface energy dominates the domain shape since $\mu \sim 0$.

The shape transformation from a networklike to a dropletlike one is induced by this competition between elastic and interfacial energy. Note that the local stress is relaxed significantly when the interconnectivity is lost. Once stress is relaxed, the interface tension makes a thin threadlike part unstable due to Rayleigh instability and it is broken up. This shape relaxation process is characterized by a speed of σ/η.

7.4. The moving droplet phase

Finally, we consider a moving droplet phase observed in polymer solutions [32]. The two important timescales characterizing the situation may be the characteristic time of the collision between two droplets (or the contact time) τ_c and the characteristic rheological time of the polymer-rich phase τ_t. Viscoelastic effects should play a role when τ_c is shorter than or comparable to τ_t. Brownian motion of a droplet with mass m is characterized by a randomly varying thermal velocity of magnitude $\langle v \rangle \sim (k_B T/m)^{1/2}$ and duration $\tau_r \sim m D_R/k_B T$ (D_R: the diffusion constant of a droplet with radius R). Thus τ_c should satisfy the relation $r_i/\langle v \rangle < \tau_c < r_i^2/D_R$, where r_i is the range of interaction. On the other hand, $\tau_t \sim \eta_s b^3 N^3 \phi^\alpha / k_B T$ [19] if we consider only topological entanglement effects. For typical values of the parameters, τ_t could be longer than τ_c for a large N or for a deep quench, especially if energetic entanglements due to attractive interactions between chains are taken into account. This means that a droplet may behave as an *elastic body* on the collision timescale for $\tau_t > \tau_c$. For $\tau_t < \tau_c$, on the other hand, droplets can coalesce with each other. This viscoelastic effect is probably responsible for the slow coarsening and the unusual dependence of the coarsening rate on the quench depth. Since τ_t is strongly dependent on N and ϕ for a droplet phase, it is natural that this phase exists only for a polymer solution having a large N under deep-quench conditions. Figures 18(a) and 18(b) schematically show the elementary process of droplet collision and the resulting coalescence for the MDP and those for the usual liquidlike droplet phase, respectively. To consider the coarsening behaviour in more detail, we need information on the distribution functions of τ_c and τ_t, which are expressed as $P(\tau_t)$ and $P(\tau_c)$, respectively. The typical situations are schematically shown in figure 19. The coarsening rate may be determined by the relation between $P(\tau_t)$ and $P(\tau_c)$. For $\tau_t/\tau_c \ll 1$, the coarsening process is similar to those for usual binary liquid mixtures and described by the usual Brownian-coagulation mechanism [1]. With increase in τ_t/τ_c, the coarsening rate should become slower and finally the MDP might be kinetically stabilized for $\tau_t \gg \tau_c$. The stabilization of the MDP might be complete for the case where $\tau_t \gg \tau_c$ and $P(\tau_t)P(\tau_c) \sim 0$. Such behaviour was actually observed in mixtures of poly(vinyl methyl ether) and water and of

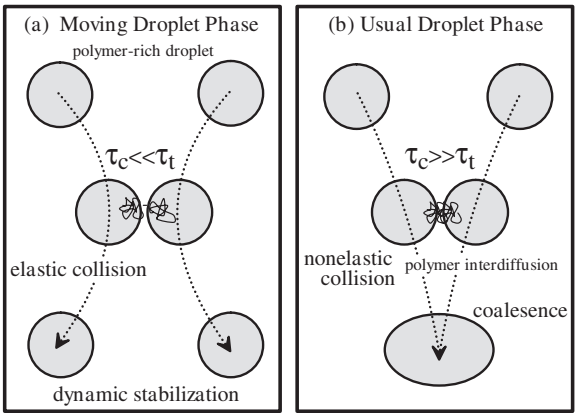

Figure 18. Schematic figures showing the elementary process of droplet collision and the resulting coalescence. (a) The MDP with dynamic stabilization of the droplet and (b) usual droplet coarsening. In case (a), polymers cannot interdiffuse between droplets during τ_c and the collision may be elastic. In case (b), on the other hand, polymers can interdiffuse between droplets within τ_c and droplets can coalesce with each other by the Brownian-coagulation mechanism.

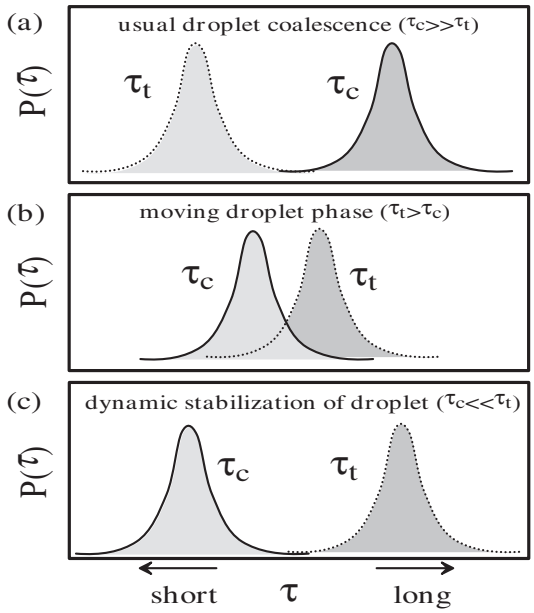

Figure 19. Schematic figures showing the relation between $P(\tau_t)$ and $P(\tau_c)$ for droplet phase separation. (a) Usual droplet phase separation; (b) the MDP with coarsening; (c) the MDP without coarsening (droplets could be dynamically stabilized.)

poly(isopropyl acryl amide) and water [29] for low polymer concentrations under deep-quench conditions. It should be noted that for these two mixtures there is a possibility that the droplets are in a physical gel state. In the stabilized MDP the size distribution of droplets was very narrow. This probably reflects the homogeneous droplet size for the initial stage of dropletlike 'spinodal' decomposition.

It is worth mentioning that the usual evaporation–condensation mechanism can play few roles in the coarsening dynamics of the MDP since vigorous Brownian motion of a droplet averages out the concentration profile around the droplet in the matrix phase within the time required for diffusion and allows no stationary, directional diffusion field to exist. This is another important factor to consider when investigating the coarsening dynamics and the stability of the MDP.

8. Numerical simulations

There are several types of simulation studies relating to viscoelastic phase separation: (a) simulations based on a solid model [73–76, 87, 88]; (b) simulations based on a two-fluid model [161–163]; and (c) molecular dynamics simulations [164]. Jäckle and co-workers [73–76] simulated phase separation of a mixture, one of whose components becomes glassy during phase separation (see figure 11(d)), using a solid model with a ϕ-dependent mobility (see section 4.1.1). They found the appearance of a more mobile phase as a droplet at the beginning of the phase separation and an unusually slow coarsening of the domain size. They also found that phase-inversion behaviour is observed for some cases [76]. The first simulation based on a two-fluid model was performed by Taniguchi and Onuki [162]. They found the formation of networklike structure. They also demonstrated that viscoelastic effects suppress hydrodynamic coarsening and slow down the domain coarsening considerably. Subsequently,

similar simulations were carried out by us, focusing on the roles of the bulk modulus in the pattern evolution, and clear phase-inversion behaviour was reproduced by a two-fluid model [161]. This study demonstrated the importance of the bulk stress, or the transient-gel formation, in viscoelastic phase separation. Bhattacharya *et al* [164] performed molecular dynamics simulations of polymer solutions, using polymer chains whose length is $N = 100$, and found networklike pattern formation. Contrary to the above-described simulations, their work did not indicate slow coarsening and they explained this by the fact that the true late-stage coarsening should be described by model H. This absence of an evident viscoelastic regime may be ascribed to the rather weak viscoelastic effects in their simulations, although we agree that the true late stage should be described by model H (see the discussion in section 6.6.2 on the order parameter switching).

Here the results of our simulation are reviewed in more detail to illustrate the importance of bulk stress. In our simulation, the effect of transient-gel formation was introduced in a rather artificial way by choosing a special composition dependence of $G_{\rm B}$ as $G_{\rm B}(\phi) = G_{\rm B}^{*}(\phi)\theta(\phi - \phi_{\rm th})$, where $G_{\rm B}^{*}$ is a smooth function of ϕ (e.g., $G_{\rm B}(\phi) \propto \phi$), θ is a step function and $\phi_{\rm th}$ is a threshold composition, below which a transient-gel state is not formed. It is assumed that $\phi_{\rm th}$ is close to an initial homogeneous composition, ϕ_0 [135, 161]. The reasons for making this assumption are as follows:

(a) It is conjectured that the network is fully stretched already at the beginning, since it is formed under the influence of strong attractive interactions between colloids and tries to shrink. Thus, it should easily be broken whenever it is strongly stretched further. This can be understood naturally with the help of the following spring model. Suppose the attractive interaction between slow components to be E. Then, the bond probability is given by $\exp[-(E - k\,\Delta x^2/2)/k_{\rm B}T]$, where k is a spring constant and Δx is an increment of the spring length with respect to its natural one. The relation $\phi_{\rm th} \sim \phi_0$ means that $E - k\,\Delta x^2/2 \sim k_{\rm B}T$ at ϕ_0. For larger E or smaller k, $\phi_{\rm th}$ is lower than the initial composition, ϕ_0. This deviation of $\phi_{\rm th}$ from the initial composition ϕ_0 may be less significant for colloidal suspensions than for polymer solutions, because of the more fragile nature of colloidal gels. The fragile nature may come from the large k.

(b) Nucleation of a liquid-rich phase is thermodynamically favoured. Thus, the break-up of the interaction network is aided by the formation of a liquid-rich phase and vice versa. Further, the above functional form of $G_{\rm B}(\phi)$ can express the sudden change of G from $G \cong 0$ to that of a transient gel, $G = G_{\rm tg}$, just after the quench. However, it is evidently artificial and a relevant microscopic theory of transient-gel formation is highly desirable.

Figure 20 shows the simulated pattern-evolution dynamics of viscoelastic phase separation without bulk and shear moduli (a), with a bulk modulus and without a shear modulus (b), without a bulk modulus and with a shear modulus (c), and with both bulk and shear moduli (d). All of these simulations were done using the same parameters. Only when there is a bulk relaxation modulus ((b) and (d)) is phase inversion observed. Note that the simulation results with both bulk and shear moduli (see figure 20(d)) recover almost all of the essential features of viscoelastic phase separation observed experimentally [30, 33]:

(i) the existence of an incubation time for nucleation of the solvent holes and their nucleation–growth-like appearance;
(ii) the volume shrinking of the polymer-rich phase (see also figure 21);
(iii) the resulting formation of a networklike structure; and
(iv) the final relaxation of the pattern dominated by the elastic energy to that dominated by interfacial tension, which leads to phase inversion.

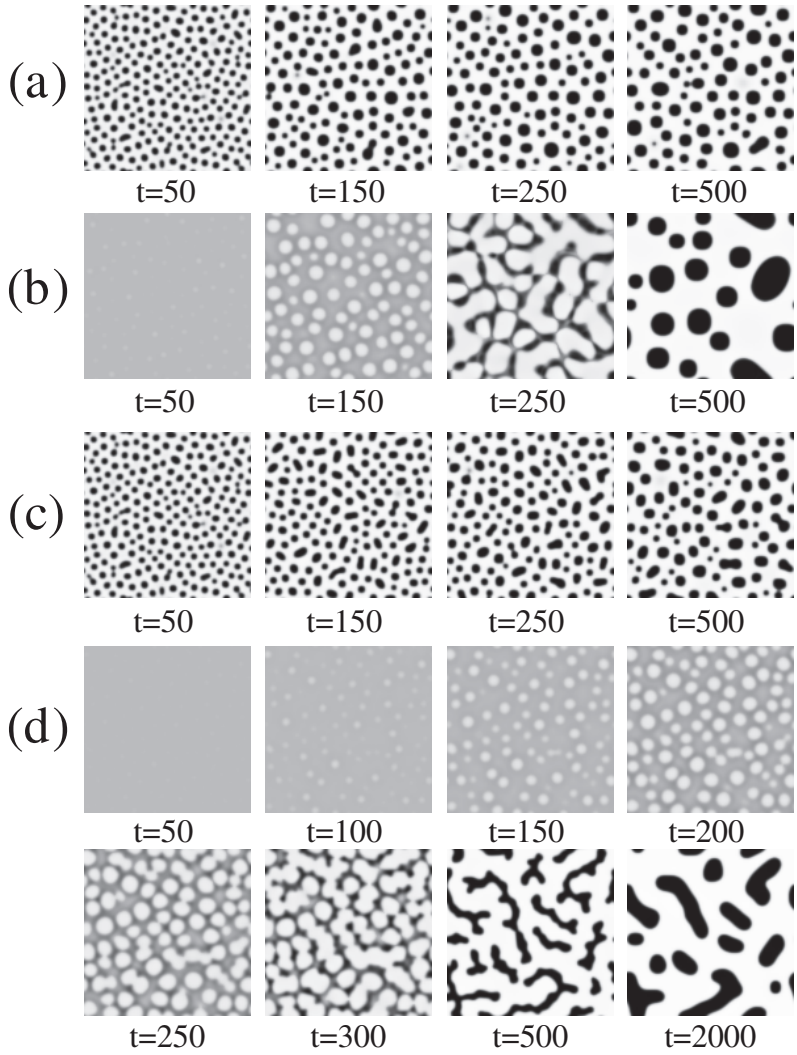

Figure 20. Simulated pattern evolution during viscoelastic phase separation: (a) without bulk and shear moduli; (b) with a bulk modulus and without a shear modulus; (c) without a bulk modulus and with a shear modulus; (d) with both bulk and shear moduli. Note that the degree of darkness is proportional to ϕ.

However, it should be noted that the spatial scale of the domain structure is much larger in the experiments than in the simulations.

Figure 21 shows the temporal change in the volume fraction Φ_p of a polymer-rich phase for all three cases. The temporal change in the degree of darkness of a polymer-rich phase even after the formation of a sharp interface in figures 20(b) and 20(d) is another indication of volume shrinking. The volume-shrinking behaviour is observed only for the cases where bulk stress exists. It is evident that the bulk stress plays a key role in the volume-shrinking behaviour and the resulting phase inversion.

Figure 22 shows the temporal change in the average magnitudes per lattice of the three types of force, namely, the osmotic stress force $\boldsymbol{F}_\phi = -\boldsymbol{\nabla}\cdot\boldsymbol{\Pi}$, the bulk stress force, $\boldsymbol{F}_B = -\boldsymbol{\nabla}\cdot\boldsymbol{\sigma}_B$,

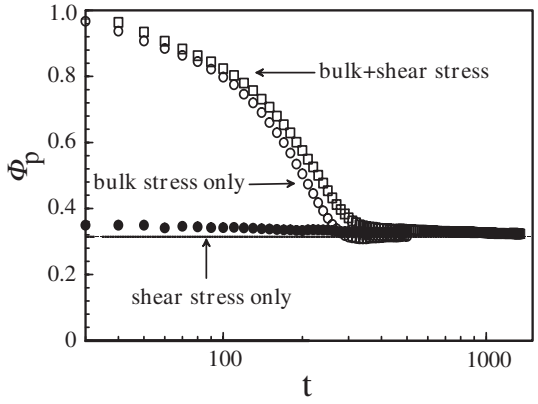

Figure 21. Temporal change in the volume (area) fraction Φ_p of a polymer-rich phase. The dotted line gives the equilibrium value of $\Phi_p = 0.309$.

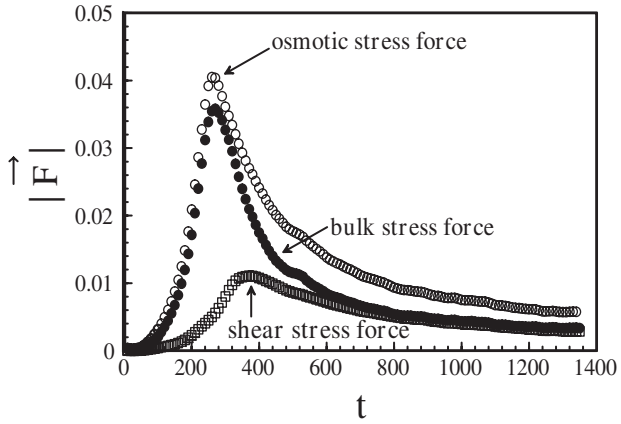

Figure 22. Temporal changes in the average magnitudes of the three types of force, $|\boldsymbol{F}|$, for case (d) in figure 20: open circles: $|\boldsymbol{F}_\phi|$; filled circles: $|\boldsymbol{F}_S|$; open squares: $|\boldsymbol{F}_B|$.

and the shear stress force, $\boldsymbol{F}_S = -\boldsymbol{\nabla} \cdot \boldsymbol{\sigma}_S$. $|\boldsymbol{\nabla} \cdot \boldsymbol{\Pi}|$ and $|\boldsymbol{\nabla} \cdot \boldsymbol{\sigma}_B|$ have peaks at the same time, $t = 270$. This is natural since both quantities are directly related to $\boldsymbol{\nabla} \cdot \boldsymbol{v}_p$. In the initial stage, these two effects are cancelled out and the diffusion is significantly suppressed. On the other hand, $|\boldsymbol{\nabla} \cdot \boldsymbol{\sigma}_S|$ has a peak at $t = 370$, retarded from the peaks of $|\boldsymbol{\nabla} \cdot \boldsymbol{\Pi}|$ and $|\boldsymbol{\nabla} \cdot \boldsymbol{\sigma}_B|$ by $\Delta t \sim 100$. Note that $\boldsymbol{\nabla} \cdot \boldsymbol{\sigma}_S$ is not directly coupled with diffusion coming from the diagonal part of $\boldsymbol{\Pi}$ and simply produces the mechanical force fields.

Figure 23 shows the temporal change in the shear relaxation time τ_S, the bulk relaxation time τ_B and the characteristic domain deformation time τ_d as well as the characteristic deformation rate $|\kappa_{ij}|$ (see equation (39) for its definition) and $|\boldsymbol{\nabla} \cdot \boldsymbol{v}_p|$. This supports the concept of order parameter switching (see figure 17).

Finally, we show the simulation results for three dimensions (3D). 3D simulations provide us with the topological or geometrical characteristics of the patterns formed during viscoelastic phase separation. The geometrical characteristics of the spongelike structure are particularly interesting. In particular, for a near-critical mixture, further, a phase inversion takes place. The preliminary simulation results are shown in figure 24. The basic features are essentially the

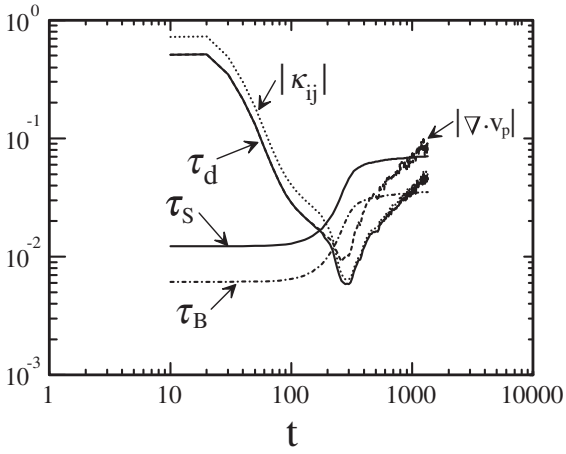

Figure 23. Temporal changes in the characteristic timescales, τ_S, τ_B and τ_d, the characteristic deformation rate, $|\kappa_{ij}|$, and $|\nabla \cdot v_p|$ for case (d) in figure 20.

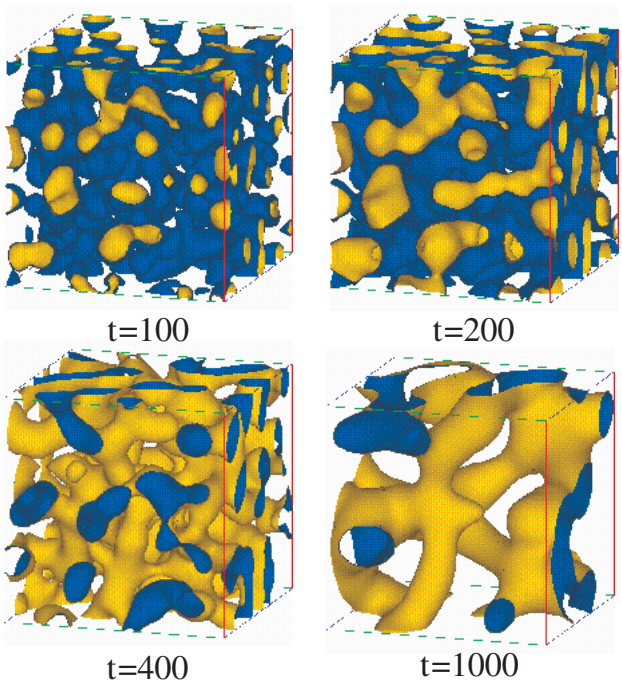

Figure 24. Temporal changes in the phase-separation pattern during viscoelastic phase separation in 3D. The pattern at $t = 1000$ is an asymmetric bicontinuous pattern, where the volume fraction of the polymer-rich (shaded) phase is significantly lower than that of the solvent-rich (transparent) phase. Later, this spongelike structure relaxes to a droplet structure to minimize the interfacial energy.

same as those for 2D. In 3D, the morphological transition can be characterized by the mean and Gaussian curvature, and the Euler number. The average Gaussian curvature changes its sign twice in the order +, −, +, reflecting the morphological transitions in the order solvent droplet,

bicontinuous sponge, polymer droplet structures, respectively. The average mean curvature, on the other hand, changes its sign from + to −, reflecting the phase inversion. The details of the study will be published in the near future [165].

These simulation results support our discussion on the mechanisms of viscoelastic phase separation. However, the effects of transient-gel formation were introduced rather phenomenologically or artificially in the above simulation. To understand the formation of a transient process, we need microscopic or mesoscopic simulations [136, 164].

9. Further examples of viscoelastic phase separation: pattern evolution governed by the elastic force-balance condition

9.1. Applications in materials science

There are a number of examples of pattern formation in materials science, which may be explained by the viscoelastic model. Some are mentioned below.

9.1.1. Polymerization-induced phase separation. Recently polymerization-induced phase separation has attracted increasing attention from both fundamental and industrial viewpoints [3, 166]. The origin of the phenomenon is very simple: suppose that there is a homogeneous mixture of two liquids. If we initiate the polymerization of one of the components by means of light or heat, the contribution of the mixing entropy significantly decreases as the polymerization proceeds. Polymerization effects can be included in the theory as a temporal change in the degree of polymerization N_A of the polymerized component A. According to the Flory–Huggins mean-field theory, the mixing free energy f can be given by

$$f(\phi, t) = \frac{1}{N_A(t)}\phi \ln \phi + \frac{1}{N_B}(1-\phi)\ln(1-\phi) + \chi\phi(1-\phi). \tag{64}$$

In some cases, the mixture finally becomes unstable and starts to phase separate even for a fixed temperature since the contribution of the entropy of mixing decreases with increase in N_A.

It is known that polymerization-induced phase separation often results in networklike or spongelike structures of a minority polymerized phase. The most well known case is that of polymer-dispersed liquid-crystal films [167–170]. In particular, Amundson *et al* [169] and Nephew *et al* [170] applied confocal microscopy and revealed three-dimensional networklike and foamlike structures.

Such phenomena can be explained quite naturally by viscoelastic phase separation [34, 171]. During phase separation, one of the components is polymerized and thus this asymmetric growth of the molecular size leads to the strong dynamic asymmetry between the two components. In this polymerization-induced phase separation, the pattern evolution is strongly affected by viscoelastic effects. Since in this case a system has a fluid component, the force-balance condition determines the morphology differently from an elastic solid model (see figure 25 and the discussion in section 9.4). Pattern evolution of polymerization-induced phase separation is first strongly affected by the initial growth of dynamic asymmetry and the resulting viscoelastic phase separation. Then the structure is frozen if a crosslinking reaction proceeds simultaneously with the linear polymerization. Thus, we believe that the viscoelastic effects dominate the pattern evolution. It is predicted that a more viscoelastic phase—namely, a polymerized phase—forms a networklike or spongelike pattern during polymerization-induced phase separation [34]. In fact, such morphology is commonly observed in polymerization-induced phase separation. For the case of polymer-dispersed liquid crystals, the Frank elastic energy of liquid crystal may also aid the formation of the networklike structure of a polymer-rich phase [172]. However, we believe that the viscoelastic effects are much more dominant

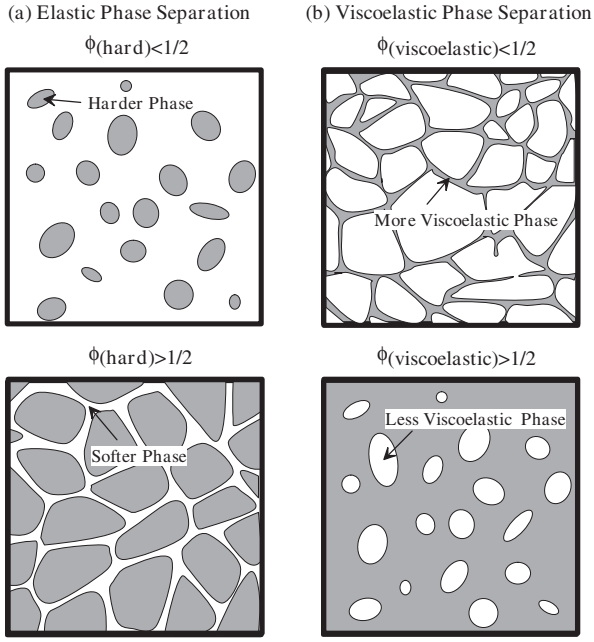

Figure 25. The difference in pattern evolution between (a) phase separation in a solid mixture with elastic deformation energy and (b) viscoelastic phase separation.

than the elastic effects. Very recently, an elastic gel growing during polymerization-induced phase separation was studied by a molecular dynamics simulation [173].

9.1.2. Membrane filters. The formation of membrane filters has been extensively studied for a long time, because of its wide applications. In many cases [174–180], the final phase-separated patterns prepared as membranes have a morphology peculiar to the intermediate stage of viscoelastic phase separation. The pattern evolution observed in the process of membrane-filter formation can also be naturally explained by viscoelastic phase separation [33, 34]. Polymeric membranes are formed from polymer solution by phase separation in most cases. In the process, phase separation of polymer solutions is induced by either evaporating a solvent or replacing a good solvent by a poor solvent (a wet process). The latter process is used in the production of viscose fibres. Once phase separation is initiated, viscoelastic effects come into play and lead to the formation of networklike or spongelike structures of a polymer-rich phase, which are suitable as filters. Then the structures can be made permanent by the following methods:

(i) simultaneous evaporation of a solvent for a polymer solution during phase separation, which leads to crystallization or vitrification of polymers;
(ii) a further quench of a system below T_g or the melting point; and
(iii) a combination of other processes such as crosslinking reactions.

9.1.3. Plastic foam. It is widely known that plastic foam has a spongelike (or cell-like) structure. The process of formation of plastic foam is as follows (see, e.g., reference [181]). First, a polymer absorbing a low-boiling-point solvent is prepared. Then, its temperature is raised above the boiling point of the solvent, which induces bubble formation in a polymer

matrix. These bubbles are nucleated and grow in size, since more solvent is supplied from the polymer matrix. The total volume of a sample expands due to the liquid–gas transformation of the solvent. In this process, the pattern is dominated by the elastic force-balance condition, as in the case of viscoelastic phase separation. This is due to the strongly asymmetric stress division: gas bubbles cannot support any stress and only the polymeric phase can support the mechanical stress. In this way, the cell-like pattern is formed. Note that elastic interactions may lead to a rather regular structure. Recently the process of polyurethane-foam formation was also studied in detail by Mora *et al* and Elwell *et al* [182–184]. The process was divided into four main regions: (i) bubble nucleation, (ii) liquid foam and microphase separation, (iii) physical gelation resulting from vitrification of the hard-segment-rich phase and (iv) chemical reaction to yield the foamed copolymer. The process is a bit complicated, but its basic features may be the same as the above. It was pointed out [33, 34] that the basic physics behind these phenomena is essentially the same as that behind viscoelastic phase separation. Recently, this view was put forward on the basis of a numerical simulation [163].

In relation to this, it should be mentioned that a plastic foam with a periodic, regular structure can be made by a special preparation method (see, e.g., reference [185]), although plastic foams with disordered structures are usually formed as in viscoelastic phase separation. This may be explained by the manner of nucleation of solvent holes: only when nucleation is heterogeneously induced with a high density in a short period may a periodic sponge structure be formed by the long-range elastic interaction between solvent holes (elastically induced correlated nucleation).

9.1.4. Monodisperse polymer balls. Polymeric particles with monodisperse size have specific applications, particularly in pharmacology and chromatography. They have been made in rather complex ways such as by successively seeded emulsion polymerization, emulsifier-free polymerization and dispersion polymerization. There are some reports on a simple way of forming monodisperse polymer particles by using phase separation of dilute or semidilute solutions of polymers [186–189]. This method is much simpler than the above-mentioned conventional techniques. However, its mechanism has not been clarified so far. We propose that the formation of monodisperse particles can be explained by the physical mechanism stabilizing the moving droplet phase (MDP). As mentioned before, the MDP is characterized by the monodisperse size of the particles and its unusual stability [28, 29, 32], which may be necessary conditions for creating monodisperse particles from a polymer solution using phase separation. Deeper understanding of the MDP should provide useful physical information on how to control the size and its distribution.

9.2. Roles of viscoelastic phase separation in Nature

Finally, we point out the possibility that spongelike structures in Nature might be associated with viscoelastic phase separation. Although there is no firm evidence, we give two examples indicating such possibilities.

9.2.1. Large-scale structures in the universe. It was pointed out [33, 34] that there is a similarity between these patterns in condensed matter and the spongelike structure of the universe (the large-scale galaxy distribution) [190]. It was speculated that the gravitational attractive interaction, which is stronger between heavier materials, acts in a similar manner to the elastic interaction network in condensed matter and produces the spongelike large-scale structure. This explanation seems to be consistent with a standard picture of the evolution of the universe (a gravitational-instability model) wherein such a heterogeneous structure develops

by gravitational amplification of density fluctuations. The details of this analogy will be discussed elsewhere. Although the above argument might be too speculative, it provides an intuitive explanation of the pattern evolution in the universe.

9.2.2. Phase separation in magma. Recently, Lucido [191] suggested that the texture of Sicilian magma may be explained by colloidal aggregation (or phase separation). He showed that it is possible that the Sicilian magma split into two liquid portions, one (basaltic) enriched in high-charge ions like iron, magnesium and calcium and the other (felsic) enriched in elements (Si, Al, Na and K) having the tendency to concentrate in the networklike structure. Such a texture might be explained by viscoelastic phase separation of magma and the freezing of a transient networklike structure by solidification, provided that there is a large difference between the rheological properties of the two phases.

9.3. Generality of sponge structure and its viscoelastic origin

As described above, there are a number of examples of pattern evolution whose characteristics can be explained by the physical mechanism of viscoelastic phase separation. The common features of these varieties of pattern formation are considered below in order to extract the universal nature underlying these phenomena.

First we discuss the universal nature of a spongelike morphology (or the formation of a continuous structure by a minority phase) and its physical origin. It is known that gel undergoing a volume-shrinking phase transition forms a bubble-like structure [56–58]. The competition between phase separation and gelation or glass transition also causes spongelike morphology [65–86]. The physical origin of the appearance of a honeycomb structure in plastic foams (e.g., polystyrene foam and urethane foam) is also similar to viscoelastic phase separation [181, 185].

All these processes have a few common features:

(i) A mixture contains a fluid as one of the components.
(ii) Holes of a less viscoelastic fluid phase (gas in plastic foam, water in gel, solvent in polymer solution and so on) are nucleated to minimize the elastic energy associated with the formation of a heterogeneous structure in an elastic medium.
(iii) Then, a more viscoelastic phase decreases its volume with time. This volume-shrinking process is dominated by the transfer (diffusion or flow) of a more mobile component under stress fields, from a more viscoelastic phase to a less viscoelastic phase.

The above picture suggests the possibility that a spongelike structure is the *universal morphology* for phase separation of any mixture in which only one component asymmetrically has *elasticity stemming from either topological connectivity or attractive interaction* and the stress is asymmetrically divided between the components.

This universal appearance of sponge structures in the phase separation of these systems originates from volume phase transition, or more strictly elastic phase separation of a *dynamically asymmetric mixture that is composed of a network-forming component and a fluid (such as a liquid and a gas)*. The elastic network can be a real one as in gels (the permanent network) or a transient network due to attractive interactions as in polymer solutions. In the former case, the real structure having large numbers of internal degrees of freedom can store the elastic energy for the 'selective' compression of the network-forming component, while in the latter case the virtual network due to long-range or short-range attractive interactions can itself store the elastic energy. In this sense, it may be concluded that the existence of both a component having a bulk (relaxation) modulus and a fluid component is a prerequisite for the

formation of a spongelike structure due to the volume shrinking of one phase. In the common-sense view of conventional phase separation, a minority phase never forms a continuous phase and forms only an isolated phase [1]. By using viscoelastic phase separation, however, we can intentionally form a spongelike continuous structure of the minority phase of a more viscoelastic phase for any dynamically asymmetric mixture.

9.4. The difference between elastic effects in solids and viscoelastic effects in fluid or gel systems

Here it is worth noting the difference [32, 34] in phase-separation morphology between elastically asymmetric solid mixtures [144] and dynamically asymmetric fluid mixtures. The difference is schematically displayed in figure 25 [32]. In the diffusion-dominated process, the system approaches the final equilibrium state to reduce the total free energy including the elastic energy (see equation (49)). As a result, the morphology that minimizes the elastic energy is selected. For example, when a softer phase is a minority phase, it forms a networklike structure since its deformation costs less energy than that of a harder phase. This is the case for solid mixtures having only elastic asymmetry and no dynamic asymmetry. Note that phase separation of elastic solid mixtures (e.g., metal alloys) does not accompany a drastic volume change of each phase if there is no strong composition dependence of the mobility. In relation to this, it should be noted that a solid mixture having a strongly composition-dependent mobility behaves quite differently (see, e.g., references [74–76]). It should be stressed, however, that this has nothing to do with elastic effects.

In the flow-dominated process, on the other hand, the force-balance condition (the Navier–Stokes equation) plays an essential role in pattern selection (see equation (42)). As a result, the morphology itself is determined by the force-balance condition. The asymmetric stress division leads to the spongelike structure where the more viscoelastic phase forms a continuous networklike structure to support the stress. Further, the two-fluid nature makes the volume change of phases possible. It is worth noting that in phase separation of a gel the morphology is determined by the force-balance condition and not by the elastic energy in the intermediate stage, even though the gel is elastic and the elastic deformation energy is included in the Hamiltonian. The final structure is, however, determined by the elastic energy. This is due to the fact that gel has a fluid component and thus the force-balance condition plays a crucial role in the selection of the morphology (see section 6.5).

10. Summary

Experiments, theories and simulations relating to viscoelastic phase separation are reviewed. It was shown that in addition to a solid and a fluid model we need a viscoelastic model of phase separation to describe phase separation of dynamically asymmetric mixtures. This model may be a general model of phase separation in isotropic condensed matter, which includes a solid and a fluid model as special cases. Thus, we can view solid and fluid models that assume dynamic symmetry between the components of mixtures as rather special cases of models of viscoelastic phase separation, contrary to common belief. Dynamic asymmetry induces a large difference in relaxation rate of the interaction networks formed by like species between the two components. This leads to the formation of a transient gel just after a quench. It is also shown that the characteristic features of viscoelastic phase separation can be well explained by the concept of 'order parameter switching' between the composition and deformation tensor. The role of a transient gel in phase-separation behaviour is discussed on a phenomenological level. The problem of transient-gel formation is closely related to the fundamental question of how the

effective free energy is expressed during a non-equilibrium process of phase separation. This problem is also connected to what the relation is between 'aggregation' and 'phase separation'. Further studies are highly desirable in order to provide an understanding of these points on a quantitative level.

Although the viscoelastic model is a quite general model of critical phenomena and phase separation, it may be intrinsically non-universal in the sense that internal slow modes of a material can affect the critical dynamics and phase-separation kinetics even near the critical point. This problem needs further studies to check whether the dynamic universality in practice breaks down in a mixture having strong dynamic asymmetry between its components or not [32, 34].

We discuss the universal features of spongelike structures observed in various materials and also in Nature, and demonstrate that there is a common physical origin that is explained by the framework of the viscoelastic model of phase separation. It is demonstrated that the most fundamental physical origin of volume-shrinking behaviour and the resulting sponge structure is the coexistence of 'asymmetry in mobility between the two components of a mixture' and 'the network-forming ability originating from attractive interactions between like species'.

Although qualitative features of viscoelastic phase separation have been understood on a phenomenological level, there still remain many fundamental problems to be solved. Deeper understanding of the phenomena is desired, to lead to a deeper understanding of pattern evolution in condensed matter and also in Nature.

References

[1] Gunton J D, San Miguel M and Sahni P 1983 *Phase Transitions and Critical Phenomena* vol 8, ed C Domb and J L Lebowitz (New York: Academic)
[2] Bray A J 1994 *Adv. Phys.* **43** 357
[3] Utracki L A 1990 *Polymer Alloys and Blends. Thermodynamics and Rheology* (Munich: Hanser)
[4] Hohenberg P C and Halperin B I 1976 *Rev. Mod. Phys.* **49** 435
[5] Snyder H and Meakin P 1983 *J. Chem. Phys.* **79** 5588
[6] Hashimoto T, Itakura M and Hasegawa H 1986 *J. Chem. Phys.* **85** 6118
Hashimoto T, Itakura M and Shimidzu N 1986 *J. Chem. Phys.* **85** 6773
[7] Bates F S and Wiltzius P 1989 *J. Chem. Phys.* **91** 3258
[8] Binder K 1991 *Material Science and Technology* vol 11, ed P Haasen (Weinheim: VCH)
Binder K 1991 *Adv. Polym. Sci.* **112** 181
[9] Hashimoto T 1993 *Materials Science and Technology* vol 12, ed E L Thomas (Weinheim: VCH)
[10] de Gennes P G 1980 *J. Chem. Phys.* **72** 4756
[11] Pincus P 1981 *J. Chem. Phys.* **75** 1996
[12] Binder K 1983 *J. Chem. Phys.* **79** 6387
[13] Onuki A 1986 *J. Chem. Phys.* **85** 1122
[14] Kawasaki K 1989 *Macromolecules* **22** 3063
[15] Hashimoto T, Takenaka M and Izumitani T 1992 *J. Chem. Phys.* **97** 679
Takenaka M, Izumitani T and Hashimoto T 1993 *J. Chem. Phys.* **98** 3528
[16] Kotnis M A and Muthukumar M 1992 *Macromolecules* **25** 1716
[17] Brown G and Chakrabarti A 1993 *J. Chem. Phys.* **98** 2451
[18] de Gennes P G 1979 *Scaling Concepts in Polymer Physics* (Ithaca, NY: Cornell University Press)
[19] Doi M and Edwards S F 1986 *The Theory of Polymer Dynamics* (Oxford: Clarendon)
[20] Hamano K, Kuwahara N, Nakata N and Kaneko M 1977 *Phys. Lett.* A **63** 121
[21] Kuwahara N, Tachikawa M, Hamano K and Kenmochi Y 1982 *Phys. Rev.* A **25** 3449
[22] Nose T 1982 *Polym. J.* **14** 289
[23] Hamano K, Tachikawa M, Kenmochi Y and Kuwahara N P 1982 *Phys. Lett.* A **90** 425
[24] Lal J and Bansil R 1991 *Macromolecules* **24** 290
[25] Kuwahara N and Kubota K 1992 *Phys. Rev.* A **45** 7385
[26] Larson R G 1999 *The Structure and Rheology of Complex Fluids* (Oxford: Oxford University Press)
[27] Haas C K and Torkelson J M 1995 *Phys. Rev. Lett.* **75** 3134

Haas C K and Torkelson J M 1997 *Phys. Rev.* E **100** 5323
[28] Tanaka H and Nishi T 1988 *Japan. J. Appl. Phys.* **27** L1787
[29] Tanaka H 1992 *Macromolecules* **25** 6377
[30] Tanaka H 1993 *Phys. Rev. Lett.* **71** 3158
[31] Tanaka H and Miura T 1993 *Phys. Rev. Lett.* **71** 2244
[32] Tanaka H 1994 *J. Chem. Phys.* **100** 5323
[33] Tanaka H 1996 *Phys. Rev. Lett.* **76** 787
[34] Tanaka H 1997 *Phys. Rev.* E **56** 4451
[35] Langer J S, Bar-on M and Miller H D 1975 *Phys. Rev.* A **11** 1417
[36] Kitahara K and Imada M 1978 *Prog. Theor. Phys. Suppl.* **64** 65
[37] Kitahara K, Oono Y and Jasnow D 1988 *Mod. Phys. Lett.* B **2** 765
Yeung C, Rogers T, Hernandez-Machado A and Jasnow D 1992 *J. Stat. Phys.* **66** 1071
[38] Puri S, Binder K and Dattagupta S 1992 *Phys. Rev.* B **46** 98
Puri S, Parekh N and Dattagupta S 1994 *J. Stat. Phys.* **75** 839
Puri S 1996 *Physica* A **224** 101
Puri S, Bray A J and Lebowitz J L 1997 *Phys. Rev.* E **56** 758
[39] Shiwa Y 1988 *Physica* A **148** 414
[40] Lacasta A M, Hernandez-Machado A, Sancho J M and Toral R 1992 *Phys. Rev.* B **45** 5276
[41] Onuki A 1992 *Phase-Transition Dynamics* (Tokyo: Iwanami) (in Japanese)
[42] Lifshitz I M and Slyozov V V 1961 *J. Phys. Chem. Solids* **19** 35
[43] Wagner C 1961 *Z. Electrochem.* **65** 581
[44] Kawasaki K and Ohta T 1983 *Physica* A **118** 175
[45] Kawasaki K 1977 *Prog. Theor. Phys.* **57** 826
[46] Siggia E D 1979 *Phys. Rev.* A **20** 595
[47] Binder K and Stauffer D 1976 *Adv. Phys.* **25** 343
[48] Ohta T 1984 *Ann. Phys., NY* **158** 31
[49] Tanaka H 1994 *Phys. Rev. Lett.* **72** 1702
[50] Tanaka H 1996 *J. Chem. Phys.* **105** 10 099
[51] Tanaka H 1997 *J. Chem. Phys.* **107** 3734
[52] Kumaran V 1998 *J. Chem. Phys.* **109** 7644
[53] Joanny J F and Leibler L 1978 *J. Physique* **39** 951
[54] Leibler L 1982 *Macromolecules* **15** 1283
[55] Tanaka H, Hayashi T and Nishi T 1986 *J. Appl. Phys.* **59** 3627
Tanaka H, Hayashi T and Nishi T 1989 *J. Appl. Phys.* **65** 4480
[56] Matsuo E S and Tanaka T 1988 *J. Chem. Phys.* **89** 1695
[57] Sekimoto K, Suematsu N and Kawasaki K 1989 *Phys. Rev.* A **39** 4912
[58] Li Y, Li C and Hu Z 1994 *J. Chem. Phys.* **100** 4637
[59] Onuki A 1993 *Advances in Polymer Sciences* vol 109 (Berlin: Springer) p 63
[60] Onuki A and Puri S 1999 *Phys. Rev.* E **59** R1331
[61] Polios I S, Soliman M, Lee C, Gido S P, Schmidt-Rohr K and Winter H H 1997 *Macromolecules* **30** 4470
[62] Vlassopoulos D, Koumoutsakos A, Anastasiadis S H, Hatzikiriakos S G and Englezos P 1997 *J. Rheol.* **41** 739
[63] Mecke K R and Sofonea V 1997 *Phys. Rev.* E **56** R3761
Sofonea V and Mecke K R 1999 *Eur. Phys. J.* B **8** 99
[64] Jinnai H, Nishikawa and Hashimoto T 1999 *Phys. Rev.* E **59** 2554
[65] Binder K, Frisch H L and Jäckle J 1986 *J. Chem. Phys.* **85** 1505
[66] Frank F C and Keller A 1988 *Polym. Commun.* **29** 186
[67] Hikmet R M, Callister S and Keller A 1988 *Polymer* **29** 1378
Callister S, Keller A and Hikmet R M 1990 *Makromol. Chem., Makromol. Symp.* **39** 19
[68] Arnauts J, Berghmans H and Koningsveld R 1993 *Makromol. Chem.* **194** 77
Berghmans S, Mewis J M, Berghmans H and Meijer H 1995 *Polymer* **36** 3085
[69] Meier G, Vlassopoulos D and Fytas G 1995 *Europhys. Lett.* **30** 325
[70] Karatasos K, Vlachos G, Vlassopoulos D and Fytas G 1998 *J. Chem. Phys.* **108** 5997
[71] Graham P D, Pervan A J and McHugh A J 1997 *Macromolecules* **30** 1651
[72] Barton B F, Graham P D and McHugh A J 1998 *Macromolecules* **31** 1672
[73] Jäckle J and Pieroth M 1988 *Z. Phys.* B **72** 25
[74] Sappelt D and Jäckle J 1997 *Europhys. Lett.* **37** 13
[75] Sappelt D and Jäckle J 1997 *Physica* A **240** 453
[76] Sappelt D and Jäckle J 1998 *Polymer* **39** 5253

[77] Tanaka T, Swislow G and Ohmine I 1979 *Phys. Rev. Lett.* **42** 1556
[78] Domszy R C, Alamo R, Edwards C O and Mandelkern L 1986 *Macromolecules* **19** 310
[79] Jelich L M, Numes S P, Paul E and Wold B A 1987 *Macromolecules* **20** 1943
[80] Tanaka F and Matsuyama A 1989 *Phys. Rev. Lett.* **62** 2759
[81] Mutin P H, Guenet J M, Hirsch E and Candau S J 1988 *Polymer* **29** 30
[82] Guenet J M, Klein M and Menelle A 1989 *Macromolecules* **22** 493
[83] Bansil R, Lal J and Cavalho B L 1992 *Polymer* **33** 2961
[84] Glotzer S C, Gyure M F, Sciortino F, Coniglio A and Stanley H E 1994 *Phys. Rev.* E **49** 247
[85] Sciortino F, Bansil R, Stanley H E and Alstrom P 1993 *Phys. Rev.* E **47** 4615
[86] Loren N, Langton M and Hermansson A M 1999 *Food Hydrocolloids* **13** 185
[87] Ahluwalia R 1999 *Phys. Rev.* E **59** 263
[88] Vladimirova N, Malagoli A and Mauri R 1998 *Phys. Rev.* E **58** 7691
[89] Frisch H L 1964 *J. Chem. Phys.* **41** 3679
[90] Jäckle J and Frisch H L 1985 *J. Polym. Sci., Polym. Phys. Edn* **23** 675
[91] Jäckle J and Frisch H L 1986 *J. Chem. Phys.* **85** 1621
[92] de Gennes P G 1976 *Macromolecules* **9** 587
de Gennes P G 1976 *Macromolecules* **9** 594
[93] Brochard F and de Gennes P G 1977 *Macromolecules* **10** 1157
Brochard F 1983 *J. Physique* **44** 39
[94] Tanaka T and Filmore D J 1979 *J. Chem. Phys.* **70** 1214
[95] Akcasu A Z 1989 *Macromolecules* **22** 3682
[96] Helfand E and Frederickson G H 1989 *Phys. Rev. Lett.* **62** 2648
[97] Ji H and Helfand E 1995 *Macromolecules* **28** 3869
[98] Onuki A 1989 *Phys. Rev. Lett.* **62** 2427
Onuki A 1990 *J. Phys. Soc. Japan* **59** 3423
[99] Doi M 1990 *Dynamics and Patterns in Complex Fluids* ed A Onuki and K Kawasaki (Berlin: Springer) p 100
[100] Doi M and Onuki A 1992 *J. Physique* II **2** 1631
[101] Milner S T 1993 *Phys. Rev.* E **48** 3674
[102] Dzyaloshinskii I E and Volovick G E 1980 *Ann. Phys., NY* **125** 67
[103] Holm D D and Marsden J E 1983 *Physica* D **4** 394
[104] Grmela M 1988 *Phys. Lett.* A **130** 81
[105] Sun T, Balazs A C and Jasnow D 1997 *Phys. Rev.* E **55** R6344
[106] Onuki A 1997 *J. Phys.: Condens. Matter* **9** 6119
[107] Landau L D and Lifshitz I M 1970 *Theory of Elasticity* (Oxford: Pergamon)
[108] Tanaka H 1997 *Prog. Theor. Phys. Suppl.* **126** 333
[109] Onuki A 1994 *J. Non-Cryst. Solids* **172–174** 1151
[110] Ganazzoli F, Raos G and Allegra G 1999 *Macromol. Theory Simul.* **8** 65
[111] Tanaka F and Edwards S F 1992 *Macromolecules* **25** 1516
[112] Wientjes R H W, Jongschaap R J J, Duits M H G and Mellema J 1999 *J. Rheol.* **43** 375
[113] Muratov C B 1998 *Phys. Rev. Lett.* **81** 3699
[114] Lu B, Li X, Scriven L E, Davis H T, Talmon Y and Zakin J L 1998 *Langmuir* **14** 8
[115] Russel W B, Saville D A and Schowalter W R 1989 *Colloidal Suspensions* (Cambridge: Cambridge University Press)
[116] Gast A P, Hall C K and Russel W B 1983 *J. Colloid Interface Sci.* **96** 251
[117] Lekkerkerker H N W, Poon W C K, Pusey P N, Stroobants A and Warren P B 1993 *Europhys. Lett.* **20** 559
[118] Poon W C K, Selfe J S, Robertson M B, Ilett S M, Pirie A D and Pusey P N 1993 *J. Physique* II **3** 1075
[119] Asakura S and Oosawa F 1954 *J. Chem. Phys.* **22** 1255
Vrij A 1976 *Pure Appl. Chem.* **48** 471
Mao Y, Cates M E and Lekkerkerker H N W 1995 *Physica* A **222** 10
[120] Pusey P N, Pirie A D and Poon W C K 1993 *Physica* A **201** 322
Poon W C K, Pirie A D and Pusey P N 1993 *Faraday Discuss.* **101** 322
Poon W C K, Pirie A D and Pusey P N 1995 *Faraday Discuss.* **101** 65
Poon W C K, Pirie A D, Haw M D and Pusey P N 1997 *Physica* A **235** 216
[121] Verhaegh N A M, van Duijneveldt J S, Duhont J K G and Lekkerkerker H N W 1996 *Physica* A **230** 409
[122] Verhaegh N A M 1997 *PhD Thesis* Utrecht University
[123] Verhaegh N A M, Asnaghi D, Lekkerkerker H N W, Giglio M and Cipelletti L 1997 *Physica* A **242** 104
[124] Verhaegh N A M, Asnaghi D and Lekkerkerker H N W 1999 *Physica* A **264** 64
[125] Evans R M L, Poon W C K and Cates M E 1997 *Europhys. Lett.* **38** 595

[126] Whittle M and Dickinson E 1997 *Mol. Phys.* **90** 739
[127] Soga K G, Melrose J R and Ball R C 1998 *J. Chem. Phys.* **108** 6026
[128] Soga K G, Melrose J R and Ball R C 1999 *J. Chem. Phys.* **110** 2280
[129] Lodge J F M and Heyes D M 1998 *J. Chem. Phys.* **109** 7567
[130] Mellema M, van Opheusden J H J and van Vliet T 1999 *J. Chem. Phys.* **111** 6129
[131] Carpineti M and Giglio M 1992 *Phys. Rev. Lett.* **68** 3327
Carpineti M and Giglio M 1992 *Phys. Rev. Lett.* **70** 3828
[132] Bibett J, Mason T G, Gang H and Weitz D A 1992 *Phys. Rev. Lett.* **69** 981
[133] Dickinson E and Golding M 1997 *J. Colloid Interface Sci.* **191** 166
Dickinson E and Golding M 1997 *Food Hydrocolloids* **11** 13
[134] Bourriot S, Garnier C and Doublier J-L 1999 *Int. Dairy J.* **9** 353
[135] Tanaka H 1999 *Phys. Rev.* E **59** 6842
[136] Tanaka H and Araki T, unpublished
[137] Brochard F 1988 *Molecular Conformation and Dynamics of Macromolecules in Condensed Systems* ed M Nagasawa (Berlin: Elsevier) p 249
[138] Bosse W and Kaneko Y 1995 *Phys. Rev. Lett.* **74** 4023
[139] See, e.g.,
Richert R and Blumen A (ed) 1994 *Disorder Effects on Relaxational Processes* (Berlin: Springer)
[140] Tanaka H 1996 *J. Chem. Phys.* **105** 9375
[141] Hess W and Klein R 1983 *Adv. Phys.* **32** 173
[142] Ackerson B J 1976 *J. Chem. Phys.* **64** 242
Ackerson B J 1978 *J. Chem. Phys.* **69** 684
[143] Wagner N J 1994 *Phys. Rev.* E **49** 376
[144] See, e.g.,
Cahn J W 1961 *Acta Metall.* **9** 765
Onuki A 1989 *J. Phys. Soc. Japan* **58** 3065
Onuki A and Nishimori H 1991 *Phys. Rev.* B **43** 13 649
Sagui C, Somoza A M and Desai R C 1994 *Phys. Rev.* E **50** 4865
[145] Nicolai T and Brown W 1999 *Macromolecules* **32** 2646
[146] Brown W and Stepanek P 1993 *Macromolecules* **26** 6884
[147] Wang C H, Sun Z and Huang Q R 1996 *J. Chem. Phys.* **105** 6052
[148] Berg R F and Gruner K 1994 *J. Chem. Phys.* **101** 1513
[149] Tanaka H and Nakanishi Y, unpublished
[150] Fytas G, Vlassopoulos D, Meier G, Likhtman A and Semenov A N 1996 *Phys. Rev. Lett.* **76** 3586
[151] Onuki A and Taniguchi A 1997 *J. Chem. Phys.* **106** 5761
[152] Kumaran V and Frederickson G H 1996 *J. Chem. Phys.* **105** 8304
[153] Xie Y, Ludwig K F Jr, Bansil R, Gallagher P D, Konak C and Morales G 1996 *Macromolecules* **29** 6150
[154] Müller G, Schwahn D, Eckerlebe H, Rieger J and Springer T 1996 *J. Chem. Phys.* **104** 5326
[155] Clarke N, McLeish T C B, Pavawongsak S and Higgins J S 1997 *Macromolecules* **30** 4459
[156] Onuki A 1992 *J. Physique* II **2** 1505
[157] Krishnamurthy S and Bansil R 1983 *Phys. Rev. Lett.* **50** 2010
[158] Cumming A, Wiltzius P, Bates F S and Rosedale J H 1992 *Phys. Rev.* A **22** 2147
[159] Sato H, Kuwahara N and Kubota K 1994 *Phys. Rev.* E **50** R1752
[160] Balsara A, Lin C and Hammouda B 1996 *Phys. Rev. Lett.* **77** 3847
Lefebvre A A, Lee J H, Jeon H S, Balsara N P and Hammouda B 1999 *J. Chem. Phys.* **111** 6082
[161] Tanaka H and Araki T 1997 *Phys. Rev. Lett.* **78** 4966
[162] Taniguchi T and Onuki A 1997 *Phys. Rev. Lett.* **77** 4910
[163] Sagui C, Piche L, Sahnoune A and Grant M 1998 *Phys. Rev.* E **58** 4654
[164] Bhattacharya A, Mahanti S D and Chakrabarti A 1998 *Phys. Rev. Lett.* **80** 333
[165] Araki T and Tanaka H, unpublished
[166] Kim B S, Chiba T and Inoue T 1995 *Polymer* **36** 43
[167] Drzaic P C 1995 *Liquid Crystal Dispersions* (Singapore: World Scientific)
[168] Lovinger A J, Amundson K and Davis D D 1994 *Chem. Mater.* **6** 1726
[169] Amundson K, Van Blaaderen A and Wiltzius P 1997 *Phys. Rev.* E **55** 1646
[170] Nephew J B, Nihei T C and Carter S A 1998 *Phys. Rev. Lett.* **80** 3276
[171] Tanaka H 1999 *Molecular Interactions and Time-Space Organization in Macromolecular Systems; Proc. OUMS '98* ed Y Morishima, T Norisuye and K Tashiro (Berlin: Springer) p 91
[172] Lapena A M, Glotzer S C, Langer S A and Liu A J 1999 *Phys. Rev.* E **60** R29

[173] Lee L C 1999 *Phys. Rev.* E **60** 1930
[174] Wijmans J G, Kant J and Mulder M H V 1985 *Polymer* **26** 1539
[175] Gaides G E and McHugh A J 1989 *Polymer* **30** 2118
[176] Aubert J H 1990 *Macromolecules* **23** 1446
[177] Jackson C L and Shaw M T 1990 *Polymer* **31** 1070
[178] Song S W and Torkelson M 1994 *Macromolecules* **27** 6390
[179] Kim H J, Tabe-Mohammadi A, Kumar A and Foulda A E 1999 *J. Membrane Sci.* **161** 229
[180] Matsuyama H, Berghmans S and Lloyd D R 1998 *J. Membrane Sci.* **142** 213
[181] Crevecoeur J J, Coolegem J F, Nelissen L and Lemstra P J 1999 *Polymer* **40** 3697
[182] Mora E, Artavia L D and Macosko C W 1991 *J. Rheol.* **35** 921
[183] Elwell M J, Ryan A J and Mortimer S 1994 *Macromolecules* **27** 5428
[184] Elwell M J, Ryan A J, Grunbauer H J M and Van Lieshout H C 1996 *Macromolecules* **29** 2960
[185] Widawski G, Rawiso M and Francois B 1994 *Nature* **369** 387
[186] Siegel B M, Johnson D H and Mark H 1950 *J. Polym. Sci.* **5** 111
[187] Brown H R and Wignall G 1990 *Macromolecules* **23** 683
[188] Hou W-H and Lloyd T B 1992 *J. Appl. Polym. Sci.* **45** 1783
[189] Grorelov A V, Chesne D A and Dawson K A 1997 *Physica* A **240** 443
[190] See, e.g.,
Geller M J and Huchra J P 1989 *Science* **246** 897
[191] Lucido G 1993 *Geol. Carpath.* **44** 67
Lucido G 1998 *Nuovo Cimento* D **20** 2575